Journal of Magnetism and Magnetic Materials 529 (2021) 167839

Contents lists available at ScienceDirect

Journal of Magnetism and Magnetic Materials

journal homepage: www.elsevier.com/locate/jmmm

Review Articles

Microwave absorbing properties of ferrites and their composites: A review

Anas Houbi [a,*], Zharmenov A. Aldashevich [a], Yomen Atassi [b], Z. Bagasharova Telmanovna [a], Mirzalieva Saule [a], Kadyrakunov Kubanych [a]

[a] Department of Complex Processing of Mineral Raw Materials, Faculty of Chemical Technology, Al-Farabi Kazakh National University, Almaty, Kazakhstan
[b] Department of Applied Physics, Higher Institute for Applied Sciences and Technology, Damascus, Syria

ARTICLE INFO

Keywords:
Ferrites
Permeability
Permittivity
Reflection loss
Absorption bandwidth

ABSTRACT

Recently, with the quick evolution of electronic technologies, and the development of telecommunication, high-performance microwave absorbing composites in which ferrite is one of their components have attracted a lot of attention. These composites should have high absorption intensity, a wide absorption bandwidth, a thin thickness, and finally light weightiness. These composites often exhibit efficiency to fulfill coveted magnetic and dielectric characteristics. This review provides a brief presentation of ferrites and among them are spinel ferrites and hexagonal ferrites. In addition to that, it discusses the classifications of ferrites according to magnetic properties, the synthesis methods to prepare nano ferrites, and control their properties. Also, it presents the main mechanism to absorb the microwaves (e.g. dielectric and magnetic losses) and finally discusses the microwave absorbing characteristics of ferrites and their composites in terms of matching frequency, reflection loss (RL) values, and absorption bandwidth.

1. Introduction

With the widespread use of microwaves, many researchers worked on studying the microwave absorption properties of many absorbent materials, as shown in Fig. 1 and that due to the increase in electromagnetic (EM) pollution as a result of the rapid advancement of wireless electronic devices and electronic systems and their use of high frequencies, in addition to new standards and rules relating to EM interference resulting from this kind of apparatuses [1–6]. Radar absorbing materials (RAMs) are significant means that we can use to concealment sensitive aims. Moreover, microwave absorbing materials (MAMs) applied vastly to prohibit and reduce EM reflections on great bodies like planes, tanks, and military equipment. Absorbent materials can be made in various shapes like coatings, sheets, and sponges [7,8]. At the beginning of the twenty-first century, new studies appeared in the field of microwave absorbers that focused on the preparation of novel nano ferrites such as hexagonal ferrites and spinel ferrites by introducing new doping elements into the structure of these materials and studying the effect of these dopings on their ability to absorb microwaves, as well. Researches have focused that nano ferrites can be synthesized by various techniques such as sol–gel, co-precipitation, microemulsion, etc. In order to obtain composites that have an elevated reflection loss, a wide absorption bandwidth, and a lightweight [9–13]. Scientific researches are currently focused on finding novel nanomaterials more effective to absorb microwaves. Nano ferrite constitutes one of its components of the composites, such as composite materials with a nano ferrite core and a conducting polymer shell (e.g. polyaniline (PANI), Polypyrrole (PPy), etc.), and different composite materials such as (ferrite/carbon), (ferrite/graphene), (ferrite/graphene oxide), etc. The results have shown the superior microwave absorption performance of these composites compared with nano ferrite materials alone. Furthermore, they are characterized by their lightweight and relatively low thickness.

Usually, microwave absorption behaviors of the absorbent substances are determined by complex permittivity (ε_r) which describes the interaction of the electric field with the absorbent substance and complex permeability (μ_r) which describes the interaction of the magnetic field with the absorbent substance as illustrated in equations (1,2) [14,15].

$$\varepsilon_r = \varepsilon' - i\varepsilon'' \quad (1)$$

$$\mu_r = \mu' - i\mu'' \quad (2)$$

The interaction of the electric and magnetic field with the absorbent substance occurs in two ways: stored power of the external electric and magnetic field in substance (real parts ε', μ'), lost power because of the

* Corresponding author.
E-mail address: khubi_anas@live.kaznu.kz (A. Houbi).

https://doi.org/10.1016/j.jmmm.2021.167839
Received 28 September 2020; Received in revised form 14 January 2021; Accepted 6 February 2021
Available online 20 February 2021

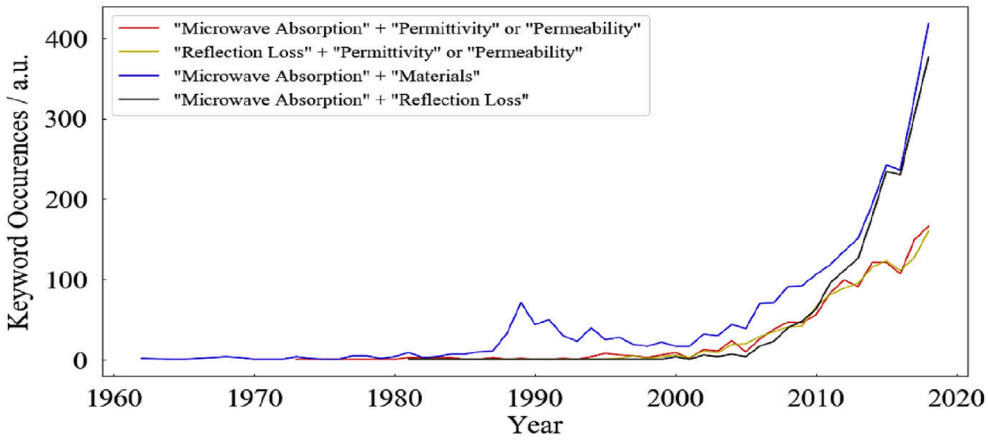

Fig 1. A curve showing the increasing trend of a number of papers reporting on microwave absorbers.

external electric and magnetic field (imaginary parts ε'', μ'') [16–18].

In addition to that, dielectric loss tangent ($tan\delta_\varepsilon$) can be represented as the ratio of both $\varepsilon'$and ε' by Eq. (3), and in the same way for the magnetic loss tangent ($\tan\delta_\mu$) Eq. (4).

$$tan\delta_\varepsilon = \frac{\varepsilon'}{\varepsilon''} \tag{3}$$

$$tan\delta_\mu = \frac{\mu'}{\mu''} \tag{4}$$

The reflection loss expressing the EM waves absorption ability can be determined by the transmission line theory, as illustrated in the following equation [19,20]:

$$Z_1 = \sqrt{\frac{\mu_r}{\varepsilon_r}}\tanh\left[j\frac{2\pi fd}{c}\sqrt{\mu_r\varepsilon_r}\right] \tag{5}$$

$$Rl = -20\log\left|\frac{Z_1 - Z_0}{Z_1 + Z_0}\right| \tag{6}$$

where Z_1 and Z_0 are material impedance and air impedance, respectively. f is the frequency of EM wave, d is the absorber thickness, and c is the velocity of light.

The mechanism of reflection loss is due to firstly the dielectric loss mechanism which happens essentially from conduction loss and polarization relaxation. The ionic polarization, electronic polarization, dipole polarization, and interfacial polarization are the main source of polarization relaxation [21–24]. According to the free-electron theory, elevated electrical conductivity (i.e., low resistivity) will promote the ε' and thus the conduct loss performs the main role in dielectric loss and polarization relaxation is small as shown in Eq. (7) [25].

$$\varepsilon' \approx \frac{1}{2\pi\rho f\varepsilon_0} \tag{7}$$

where ρ and ε_0 are the resistivity and the dielectric constant of free space, respectively.

Secondly, the magnetic loss mechanism which happens essentially from natural resonance, domain wall resonance, and eddy current effect [26–29]. The natural resonance commonly occurs at a lower frequency and is linked to the anisotropic domain [30], which can be shown using equation (8).

$$f_r = \frac{\beta H_a}{2\pi} \tag{8}$$

where f_r, H_a, andβ are the resonance frequency, the anisotropic field, and the gyromagnetic proportion, respectively.

In order to gain efficient EM wave absorption, there should be efficient integration between dielectric and magnetic losses, so as to obtain certain impedance properties. The impedance matching (Z) property of the pattern can be calculated from Eq. (9) as the following:

$$z = \frac{z_1}{z_0} \tag{9}$$

When impedance matching is equal to or near to 1, the EM waves are not reflected on the surface of the absorbent substance and are all incident within the absorbent substance. At this period, the absolute value of the RL will arrive at the maximum value.

The attenuation of electromagnetic waves within the absorbent substance is a significant part of advanced MAMs because this attenuation constant (α) defines the dissipation characteristics of the substance as shown in Eq. (10) [31].

$$\alpha = \sqrt{2}\,\pi f\left[\left(\mu_r''\varepsilon_r'' - \mu_r'\varepsilon_r'\right) + \left[\left(\mu_r''\varepsilon_r'' - \mu_r'\varepsilon_r'\right)^2 + \left(\mu_r''\varepsilon_r' - \mu_r'\varepsilon_r''\right)^2\right]^{\frac{1}{2}}\right]^{\frac{1}{2}} \tag{10}$$

It can be inferred from the attenuation constant equation that the controlling attenuation mechanisms for microwave absorption are dielectric loss and magnetic loss.

2. Purpose of the review

The purpose of this review is to present, summarize and tabulate the recent results presented in the literature for nano ferrites and their composites. In addition to that, we've highlighted the properties of spinel ferrites and hexagonal ferrites. On the other hand, we've focused on the synthetic techniques of nano ferrites and shown the advantages and disadvantages of the synthesis techniques and a discussion of the parameters impacting properties of nano ferrites.

3. Types of ferrite

Ferrites are ceramics made by blending iron (III) oxide (Fe_2O_3, rust) with small ratios of one or more additional metallic elements. Ferrite is ordinarily given by the general formula M–(Fe_xO_y), where M stands for divalent mineral ions such as (Ba, Co, Ni) [32]. Ferrites have an elevated saturation magnetization, elevated resistivity (0.1–105 Ω-m), and adjustable contrast range which give ferrites a preferred option in a broad field of applications. The magnetic properties of ferrite materials are the result of the magnetic moments related to the single electrons, where the magnetic properties of the atoms are determined by the number of single electrons around the nucleus, where every single electron contributes a magnetic moment resulting from its rotation around itself and around the nucleus. Ferrites can be divided into two groups depending on their magnetic coercivity [33–37]. Hard ferrites have distinguished high coercivity, so it is hard to demagnetize. They are

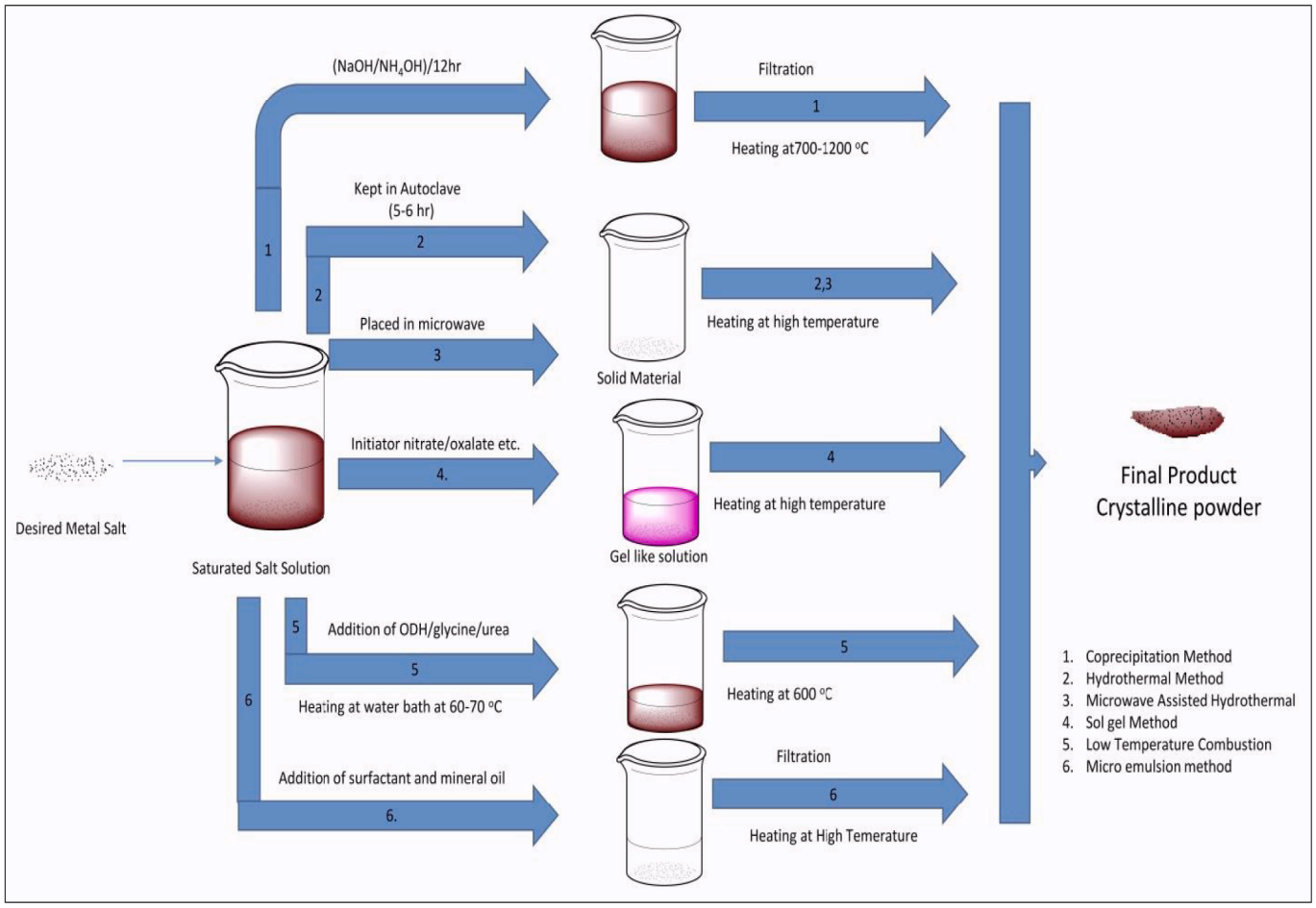

Fig 2. Graphical design of different manufacturing methods leading to nano ferrites.

used to fabricate permanent magnets for applications such as loudspeakers and small electric motors [38–40]. Soft ferrites have low distinguished coercivity (H_c), so they facilely change their magnetization and work as conductors of magnetic fields. They are used to fabricate efficient magnetic cores [41–44]. Ferrites are classified by names of common minerals that have the crystal construction to the:

3.1. Spinel ferrite

This is ordinarily given by the general formula Q–(Fe_2O_4), where tetrahedral and octahedral interstitial positions are determined with Q (divalent mineral ions such as zinc, cobalt, nickel, manganese) and iron, respectively. Given their usability in the microwave domain, spinel alloys can be utilized as MAMs, since these ferrites have low-conductivity (semiconductor particular) and high magnetic losses. But, spinel ferrites in microwave absorption uses are limited by the low resonance frequency [45,46].

3.2. Garnet ferrite

This is ordinarily given by the general formula $Re_3Fe_5O_{12}$ where Re refers to a trivalent ion for example gadolinium, dysprosium, and neodymium. This kind of ferrites has a comparable structure to the spinel ferrites however with some additional positions (dihedral axis). Garnet is a soft ferrite that has low H_c, and a large M_s. Furthermore, garnet has good chemical stability and the ability to repress EMI [47].

3.3. Hexagonal ferrite

This kind of ferrites has an elevated crystalline magnetic contrast field and flat contrast that enhances their normal resonance in the upper GHz band. This hexagonal ferrite property raises its versatility in a diversity of uses. This ferrite crystallizes into a hexagonal structure. Aside from spinel ferrites, the magnetic structure of these ferrites enables the trait to operate in the entire gigahertz band because of their high essential magnetic variance [48]. There are six kinds of hexagonal ferrites:

3.3.1. M-kind

M-kind ferrites are presented through the general formula Q-($Fe_{12}O_{19}$) where Q stands for mineral ions such as lead, barium, strontium, etc. The contrast of big magnetic crystal properties, cheap cost, elevated curie temperature (T_C), and particular M_s characteristics of these types of ferrites make them efficient microwave substances.

3.3.2. Y-kind

Y-kind ferrites are presented through the formula T_2Q_2-($Fe_{12}O_{22}$) where T stands for mineral ions such as lead, barium, strontium, and the same for the Q such as copper, zinc, cobalt, etc. This kind of ferrites is ferromagnetic substances. Hence, the addition of mineral ions in these hexaferrites will lead to dominant their magnetic properties with a view to getting the best microwave absorption [49].

3.3.3. W-kind

W-kind ferrites are obtained with the formula T_2Q_2-($Fe_{16}O_{27}$). The structures of these ferrites are linked to the M-kind. These ferrites

Table 1
Summary of the features and limitations of the main synthesis techniques.

Technique	Nanomaterial	Calcination temperature (°F)	Size (nm)	Features	Limitations	Refs.
Hydrothermal	$Mn_{1-x}Zn_xFe_2O_4$	338	15	Controlled size. High yield. Scalable.	Previous information on solubility is wanted. High pressure.	[73]
Mechano–Thermal	$ZnFe_2O_4$	248	9–20	Fine particle size.	Time-consuming.	[74]
	$MgFe_2O_4$	752–1292	5–8	Accumulation of ferric oxide.	Existence of impurities.	[75]
	$ZnFe_2O_4$	752–1022	3–20		Poor yield.	[76]
Microwave –Thermal	$BiFeO_3$	356	130	Rapid operation.	Exaggerated growth existence of impurities.	[77]
	$BiFeO_3$	752–1112	20–160	Cost-effective.		[78]
	$CoFe_2O_4$	1112–1472	11–12	They obtained a crystalline structure.		[79]
Combustion	$Zn_{1-x}Co_xFe_2O_4$	1742	30–40	Cost-effective process.	Opportunity for impurity forming.	[80]
	$CdFe_2O_4$	1742	12–27	Low-temperature wanted.	High temperature is wanted.	[81]
	$MgFe_2O_4$	932	12–25	Potentially of multi-		[82]
	$BaNi_2Fe_{16}O_{27}$	1292–1832	10–70	component. Nanoparticle forming.		[83]
Sol-Gel	$Sm_{1-x}Ca_xFeO_{3-y}$	1292–1832	100	Controlled size and form.	Expensive process.	[84]
	$Sr_{0.7}Nd_{0.3}Fe_xCo_{0.3}O_{19}$	2012	40–50	Better homogeneity.	Requests complete monitoring.	[85]
	$Mn_{1-x}Zn_xFe_2O_4$	1292–2012	500	Low cost.		[86]
	$NiFe_2O_4$	842	11–16			[87]
Co-precipitation	$NiFe_2O_4$	*	>50	Decrease in the reaction	The solubility of interactivity materials impacts	[63]
	$Mg_{0.5}Ni_{0.5}Fe_2O_4$		290–340	temperature.	the precipitation ratio.	[64]
	$CoCr_xFe_{2-x}O_4$		15–23	Aqueous media.	Poor crystallinity.	[65]
	$NiFe_2O_4$		8–20	Symmetric sized. Nanoparticle forming.	Time-consuming.	[66]
Micro Emulsion	$CoFe_2O_4$	1112	28	Single-phase nano-particles.	Temperature-dependent.	[67]
	$SrFe_{12}O_{19}$	752–1832	60	Regular crystalline structure.	Existence of impurities.	[88]
	$Ni_{0.5}Zn_{0.5}Fe_2O_4$	1112	50	Cost-effective.	Less yield.	[89]
Wet chemical	$BiFeO_3$	842–1202	50–200	Low-temperature wanted.	Poor yield.	[68]
	$Mg_{1-x}Zn_xFe_2O_4$	752–1652	100–150	Fine particle size.	Possible impurity. Contamination.	[69]
	$MnFe_2O_4$	1292–2192	14–40			[70]
Refluxing	$Ni_xZn_{1-x}Fe_2O_4$	212	14–19	Control on reaction rate. Symmetric size of particles.	Low yield. Time-consuming.	[72]

properties relied on the particle shape and the way of composition and arrangement of cations in the crystal body [50,51].

3.3.4. X-kind

X-kind ferrites are obtained with the formula T_2Q_2-($Fe_{28}O_{46}$) [52]. X-kind hexaferrites can be thought of as a blend of M and W-kind hexaferrites. Compared with M and W- kind hexaferrites, these ferrites possess bigger T_c and M_s, thus they act as the best MAMs.

3.3.5. Z-kind

Z-kind ferrites are presented through the formula T_3Q_2-($Fe_{14}O_{41}$). These hexaferrites have a perfect permeability and more elevated resonant frequency (f_r) compared to spinel ferrites. This is a reason why these ferrites are only utilized in microwave systems such as antennas, inductors and permanent magnetic applications [53].

3.3.6. U-kind

The U-kind hexaferrites are obtained with the formula T_4Q_2-($Fe_{36}O_{60}$). Among the hexaferrites, these ferrites have greater thermal stability, and high M_S [48]. Hence, this kind of ferrites has been utilized in a lot of research on Electromagnetic interference uses.

4. Synthesis techniques of nano ferrites

The way of synthesis is of most important to get the desired output as characteristics of different kinds of nano ferrites changes significantly with various techniques of synthesis. For example, the size and form of particles define the characteristics of nano ferrites, which in the turn are organized by way of synthesis. Nano ferrites can be manufactured via various techniques as shown in Fig. 2.

4.1. Thermal technique

An ideal thermal technique includes a chain of various steps for getting nano ferrites and their composites. These methodologies of synthesis involve hydrothermal, microwave-aided hydrothermal (MAH), colloid mill or mechano-hydrothermal, combustion, and thermal decomposition method techniques. Nano-particles acquired from the thermal process on the decay of organometallic precursors usually submit symmetric shape and size dispensation. Chemical reactions occur in the hydrothermal method of initial materials (mineral salts) within an aqueous medium under certain conditions of temperature and pressure. The preparation process takes place in special reactors through which the interaction conditions can be controlled to crystallize the ferrite material directly from the solution [54–57]. Some researchers have modified this method by linking it to microwaves treatment to obtain products with unique characteristics such as grain size and microscopic shape [58]. Table 1 shows the features and limitations of the thermal technique.

4.2. Sol-Gel technique

The sol–gel technique can be defined as forming a relatively stable solid phase at a specific temperature starting from the liquid phase. The main reactions in this method are the hydrolysis phase, where the acids and bases are used as catalysts, and the condensation phase. In this phase, the molecules resulting from hydrolysis are linked together to form a three-dimensional structure. The essential primary materials used in this technique are chlorides and nitrates of metals [59–61]. On the other hand, it is necessary to carefully control the variables of the sol–gel method to obtain a homogeneous final product and good magnetic and microwave absorption properties, the most important of which are: purity, quality of raw materials, reaction temperature, stirring quality (mechanical, ultrasound, and magnetism), and finally the pH

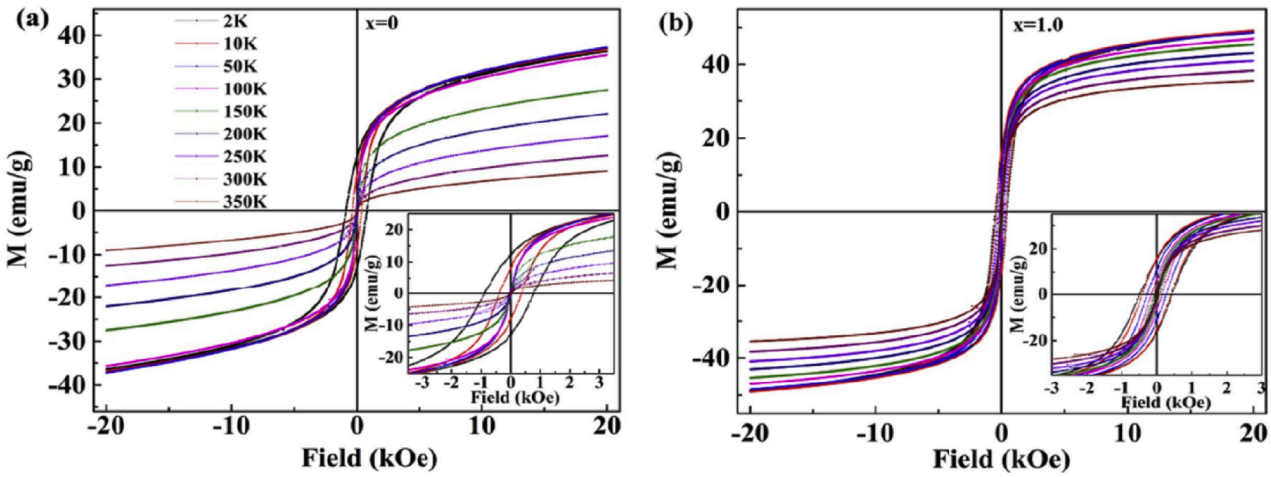

Fig 3. (a, b) Hysteresis loops have measured at various temperatures for x = 0 and x = 1 compositions.

value. Mallesh et al. prepared $Mn_xZn_{1-x}Fe_2O_4$ (x = 0–1) by sol–gel technique. The microstructure and low-temperature magnetic characteristics of ferrite nanoparticles were examined. The results showed the average particle size between 13 and 20 nm. As for the temperature and magnetic field reliance the results of magnetization, a superparamagnetic (SPM)-like conduct is shown with a big magnetic moment (~104 μ_B) in particles [62]. The hysteresis loops have obtained at various temperatures for x = 0 and x = 1 compositions as shown in Fig. 3. Table 1 shows the advantages and disadvantages of the sol–gel technique.

4.3. Co-precipitation technique

This technique is considered one of the most important to prepare ferrite nanomaterials. It mainly depends on preparing an aqueous solution based on suitable initial materials to form the ferrite, adding a convenient sedimentation factor until a convenient pH is reached, and a precipitate is obtained, followed by a filtration and drying process, and heat treatment to obtain the nano ferrite powder. Among the most significant initial materials used in this method: metal chlorides, metal nitrate, metal sulfate as sources of mineral cations, ammonium hydroxide, and sodium hydroxide as sedimentation agents [63–66]. Table 1 shows a summary of the features and limitations of the co-precipitation technique.

4.4. Microemulsion technique

The microemulsion technique is used for attaining more concern in essential as well as manufacturing research due to their unique characteristics. We mention some of them like thermodynamic stability, sizeable interfacial area, and capability to get dissolvable in immiscible liquids. The microemulsion technique includes three segments, water, oil, and surfactant. During blending organometal antecedents, a precipitate is formed. This technique controls different particle characteristics like homogeneity, geometry, morphology, and particle size. These particles are used in magnetic recording and microelectronic devices [67]. Table 1 shows the advantages and disadvantages of the microemulsion technique.

4.5. Other techniques

These kinds of techniques, like the refluxing technique, ceramic technique, wet chemical technique, etc. [68–72]. The selection of suitable synthetic techniques is of immense significance for the manufacture of nano ferrites and is collected in Table 1.

5. Parameters affecting properties of nano ferrites:

The variation in nano ferrites characteristics can be tuned by controlling the different parameters of synthesis, like the composition,

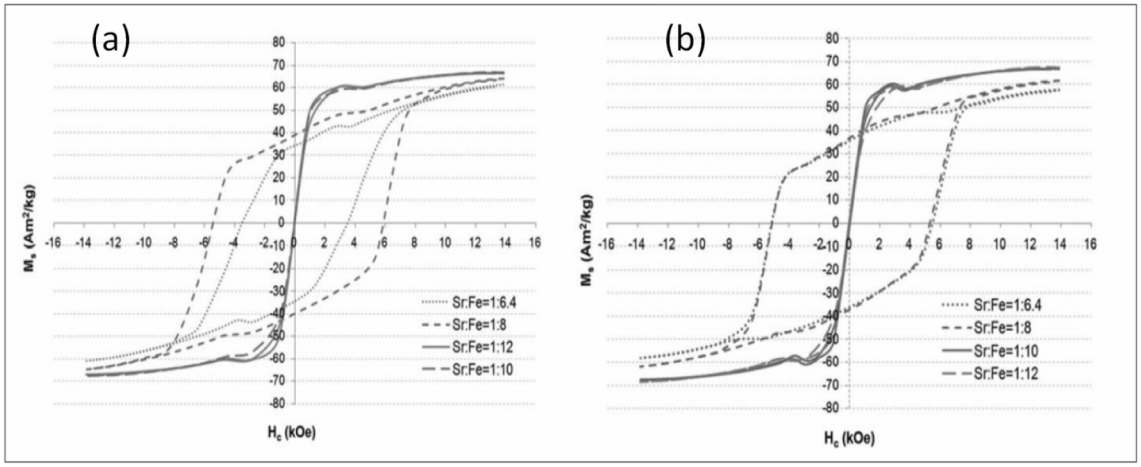

Fig 4. The hysteresis curves of $SrFe_{12}O_{19}$ manufactured by the co-precipitation technique (a) and the microemulsion technique (b) with various Sr^{2+}/Fe^{3+} mole percentage and calcined at 900 °C.

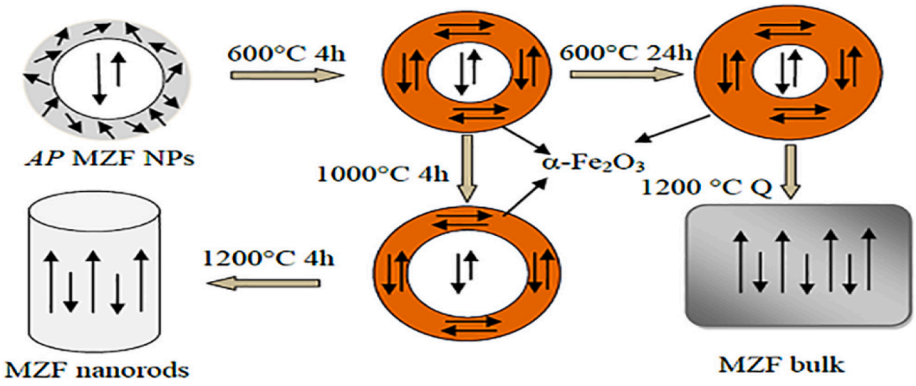

Fig 5. Phenomenological model of phase development in MZF NPs.

combustion temperature, and value of pH.

5.1. Composition

The composition of interacting materials is a significant factor for controlling the nano ferrites by changing the mole percentage of the interacting substances. Drofenik et al. prepared $SrFe_{12}O_{19}$ by the co-precipitation technique. The results referred that the reduction in the Sr^{2+}/Fe^{3+} mole percentage from 1:8 included a severe alter in magnetic conduct that appeared by an extreme variation in the hysteresis loop as shown in Fig. 4 [88].

5.2. Combustion temperature

Combustion or annealing temperature is the essential parameter that impacts the magnetic, microwave absorbing properties, and morphological nature of nanoparticles [90–93]. Mallesh et al. prepared $Mn_xZn_{1-x}Fe_2O_4$ ($0 \leq x \leq 1.0$) compositions by sol–gel method. The structure, thermal stability, and magnetic characteristics of as-prepared and annealed patterns have been studied. Though, as-prepared and 1200 °C air annealed patterns show cubic spinel ferrite phase, they crumble into α-Fe_2O_3, or/and α-Mn_2O_3 phases along with the poor quality of ferrite phase on annealing at 600 °C in the air. Fig. 5 shows the phenomenological model of phase development in MZF NPs. Present investigations show that the stability of spinel ferrite phase is sensitive to (i) Mn concentration (ii) the annealing temperature and (iii) environments (air, Oxygen, and Argon atmosphere) in which annealing experiments were executed [94]. Prabu et al. prepared the $MgFe_2O_4$ by sol–gel method and studied the structure and magnetic characteristics of Magnesium ferrite, The XRD samples of as studied and annealed nanoparticles of $MgFe_2O_4$ patterns showed pure spinel phase. But annealing at intermediate temperature (500 °C-1000 °C) outcomes in the

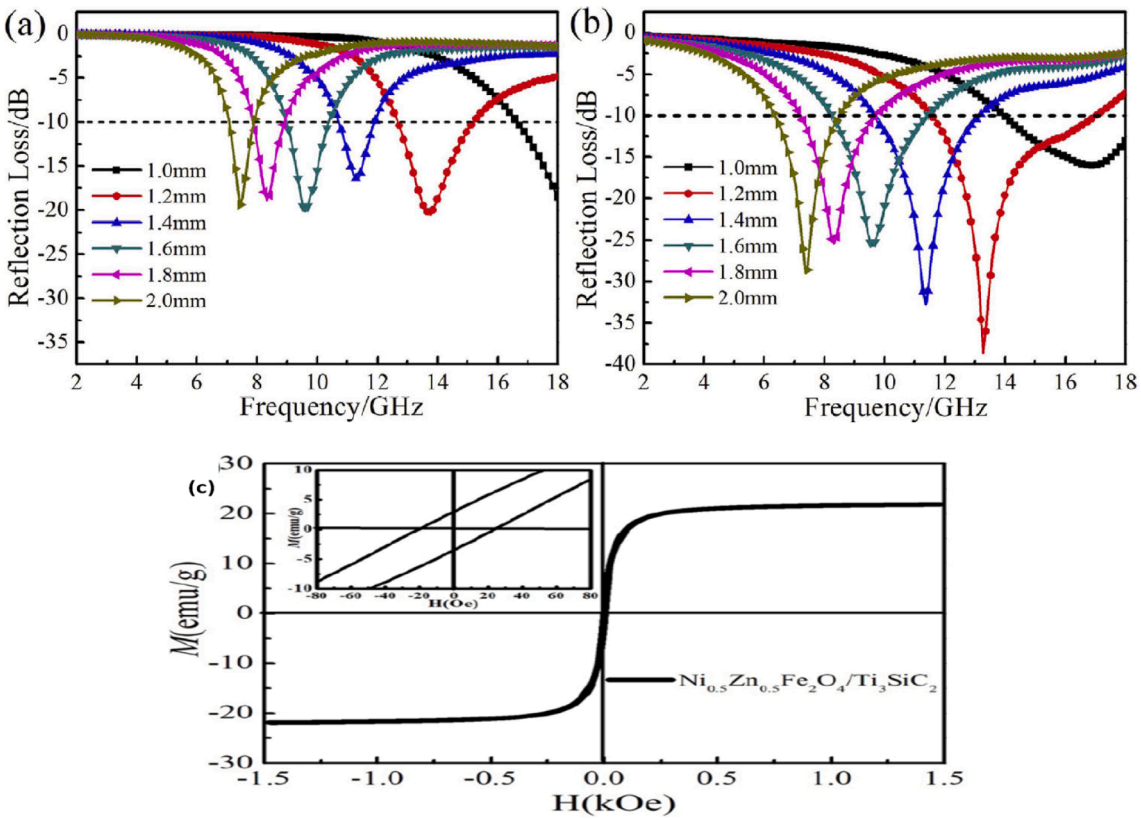

Fig 6. Measured RL of (a) Ti_3SiC_2, (b) $Ni_{0.5}Zn_{0.5}Fe_2O_4/Ti_3SiC_2$ absorbing coating with different thicknesses and (c) Hysteresis loop of the $Ni_{0.5}Zn_{0.5}Fe_2O_4/Ti_3SiC_2$ pattern, inset shows enlarged region of the loop around the origin.

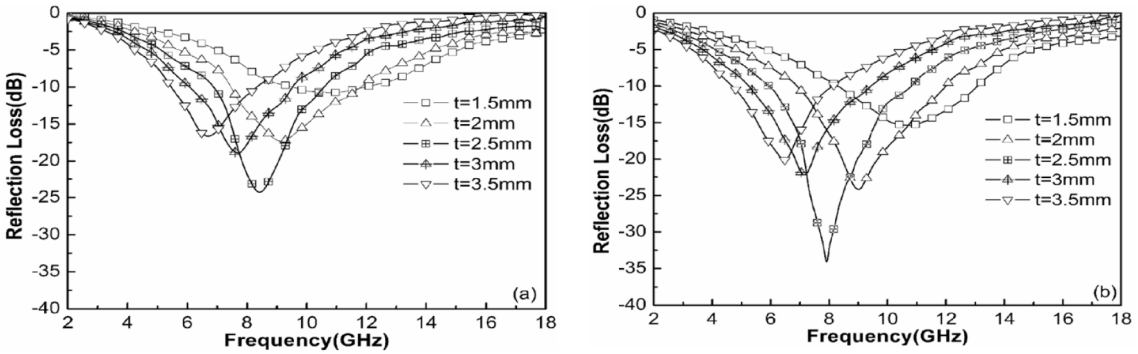

Fig 7. Frequency dependence of reflection loss of Ni $_{0.7}Zn_{0.3}Y_xFe_{2-x}O_4$ ferrite (x = 0, (a); x = 0.2, (b)) at various thicknesses.

development of α-Fe_2O_3, MgO secondary phases along with ferrite phase. This leads to the deterioration of magnetic characteristics [95].

5.3. Value of pH

The variance in pH value controls the microwave absorbing characteristics and morphologies of nanomaterials. Where the nano ferrites are immediately impacted by the pH value [96]. Huang et al. studied the Co-Zn ferrite by the co-precipitation technique at various pH situations in the field of 9–11. The results detected when the pH situation was raised from 9 to 11, the particle size for the compound reduced from 40 nm to 30 nm, the difference in microstructure considers a significant factor in dominating the EM characteristics. The magnetic loss was 0.2–0.5, and the dielectric loss was 0.02–0.07 for the compound at pH of 9, which shows significantly improved magnetic loss and dielectric loss characteristics than the patterns studied at pH of 10 and 11 [97].

6. Microwave absorbent of ferrite materials

The researchers worked to develop the absorption materials of the microwave by studying several factors and variables such as the method of preparation, the type of ferrite material, the effect of the process of substitution with different mineral cations, the thickness of the absorbent substances, etc. Luo et al. prepared the Ti_3SiC_2 particles encapsulated by $Ni_{0.5}$ $Zn_{0.5}$ Fe_2O_4 shell through the sol–gel technique, which provides the $Ni_{0.5}Zn_{0.5}Fe_2O_4/Ti_3SiC_2$ compound owning a good permittivity and coveted bigger permeability, consequencing is a better impedance matching characteristics and effective EM attenuation ability, as shown in (Fig. 6: a–b), the measured absorbing bandwidth under −10 dB was 5.3 GHz and maximum RL of −38.6 dB were obtained for the $Ni_{0.5}Zn_{0.5}Fe_2O_4/Ti_3SiC_2$ absorbing coating with a thickness of 1.2 mm. The hysteresis loop of the $Ni_{0.5}Zn_{0.5}Fe_2O_4/Ti_3SiC_2$ pattern was measured and the results were M_s and H_c were 21.82 emu/g and 33.07 Oe, respectively as shown in Fig. 6(c) [98].

Mingyuan et al. studied $Ni_{0.7}Zn_{0.3}Fe_2O_4$ and $Ni_{0.7}Zn_{0.3}Y_xFe_{2-x}O_4$ by the sol–gel method. The absorption results show when the material is thicker, that leads the matching frequency will displace towards the lower frequencies, as shown in (Fig. 7: a–b) [99]. We can be explained that the spreading wavelength in the absorbent material λ_a is given by the following relationship (11) [100–102]:

$$\lambda_a = \frac{c}{f\sqrt{|\mu_r||\varepsilon_r|}} \tag{11}$$

When the thickness of the absorbent material is equivalent to a fourth of the spreading wavelength in the absorbent material, then the reflected wave from the surface separating the two mediums (absorbent material-air) will interfere with the phase-varying wave and reflected from the surface separating the two mediums (metal-absorbent material). This thickness is called the matching thickness, and it is given by the following relationship (12) [103–105].

$$t_m = \frac{n\lambda_a}{4} = \frac{nc}{4f\sqrt{|\mu_r||\varepsilon_r|}}(n = 1, 3, 5, \cdots) \tag{12}$$

Bueno et al. prepared $Cu_{0.2}Ni_{0.4}Zn_{0.4}Fe_2O_4$ by Citrate precursor and studied the microwave absorption properties for this ferrite. The results indicated this ferrite exceeded the −10 dB threshold within the range (X-band) on a range reached to 2.4 GHz [106]. Ghosh et al. studied the same previous compound but prepared it in a different method, which was the co-sedimentation method. The results indicated this ferrite exceeded the −10 dB threshold within the range (X-band) on a range reached to 4.1 GHz with a thickness of 2.5 mm and the loading percentage 30%w/w [107]. Where the changes in microwave absorption properties were noticed with the change of the preparation method. Chen et al. prepared the spinel ferrite, which was $Ni_xCo_{1-x}Fe_2O_4$ (x = 0.5, 0.8) by ball milling. The results illustrated for $Ni_{0.8}Co_{0.2}Fe_2O_4$ that the maximum RL was −35.5 dB at the frequency of 11.5 GHz for the thickness of 2.5 mm, the absorption bandwidth under −10 dB was 3.2 GHz, the dielectric loss was ($\varepsilon_r = 9.6 + i0.13$), and the magnetic loss was (μ_r = 1- i0.3). As for $Ni_{0.5}Co_{0.5}Fe_2O_4$ that the RL was −30.6 dB at the frequency of 11.9 GHz for the thickness of 2.5 mm, the absorption bandwidth under −10 dB was 3.4 GHz, the dielectric loss was ($\varepsilon_r = 8.3 + i0.25$), and the magnetic loss was (μ_r = 0.7- i0.3) [108]. Where the changes in microwave absorption properties were observed with the change of the compound composition, as mentioned above.

On the other hand, other researchers have studied the effect of the process of substitution with a number of mineral cations and substitution rates on ferrite. Almessiere et al. prepared $[Ni_{0.4}Cu_{0.2}Zn_{0.4}](Nd_xY_xFe_{2-2x})O_4$ (x ≤ 0.05) with partly Nd/Y replaced by citrate sol–gel auto-combustion method. The magnetic proprieties were studied for specimens at temperature 300 K, where the hysteresis loops for the specimens that are non-substituted (x = 0) showed superparamagnetic conduct, whereas the specimens which Nd-Y substituted NiCuZn ferrite showed soft ferrimagnetic status. It was noticed that the volume of magnetization decreases with an increase in Nd^{3+} and Y^{3+}amounts. ZFC–FC magnetic measurements detected the presence of dipolar reactions, which illustrate a partly blocked case in conformity with hysteresis loops at temperature 300 K. For all tested $[Ni_{0.4}Cu_{0.2}Zn_{0.4}](Nd_xY_xFe_{2-2x})O_4$ (x ≤ 0.05) NSFs, the maximum intense absorption was noticed at the frequencies of 2.49–4.15 GHz. The maximum RL −44.69 dB was noticed [109]. Slimani et al. prepared $Ni_{0.4}Cu_{0.2}Zn_{0.4}Tb_xFe_{2-x}O_4$ (0.0 ≤ x ≤ 0.10) by sonochemical method. The NSFs structure was verified by XRD test. In addition to that, the microstructural was investigated by SEM device. The results showed that the substitutions rate gave a substantial impact on dielectric characteristics, whereas ion substitution has limited however a distinguished impact on AC/DC conductivity variation. Finally, the appearances of the EM absorption in the field of 1.8–3.8 GHz were noticed [110]. Almessiere et al. prepared the partly Eu substituted $Ni_{0.4}Cu_{0.2}Zn_{0.4}Eu_xFe_{2-x}O_4$ (0.0 ≤ x ≤ 0.10) nanostructured spinel ferrites (NSFs) via sol–gel auto-combustion technique. The XRD analyses confirmed the presence of the single-phase

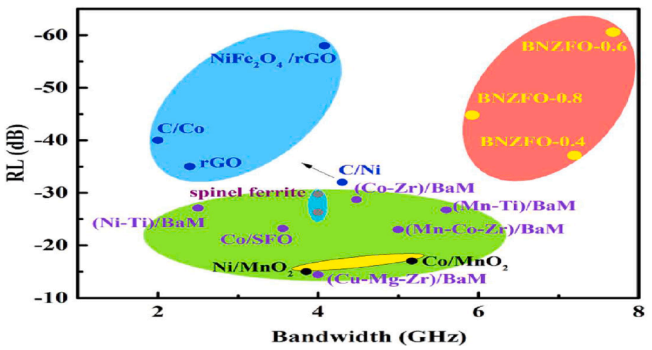

Fig 8. The comparing of the absorption characteristics got in this research with those in other researches.

structure in all the studied patterns. The paramagnetic contribution of the NSFs rose with the increase in Eu^{3+} contents. The frequency dispersals of the permeability and permittivity were used to define the RL in the 1 to 20 GHz frequency field [111]. Slimani et al. studied the dysprosium ions (Dy^{3+})-substituted NFs of compound $[Ni_{0.5}Co_{0.5}](Dy_xFe_{2-x})O_4$ ($x \leq 0.08$) utilizing the citrate gel method. All the NFs referred that the absorption of the EM radiation was in the frequency range 2.9–5.5 GHz because of the ferromagnetic resonance. It's been confirmed that by dominating the Dy^{3+} contents accurately, the MA and magnetic properties of the suggested spinel NFs can be designed [112]. From these studies were observed that the non-substituted ferrites were distinguished by their modest ability to absorb microwaves, which necessitated the search for the effect of the process of substitution with a number of mineral cations and substitution rates on ferrite through which the microwave absorption and magnetic properties were improved, as the tests result indicated.

On the other hand, other researchers have studied the effect of Doped on microwave absorption properties. Bai et al. studied the Ni^{2+}-Zr^{4+}Co Doped barium ferrite ceramics, the results showed that $BNZFO_{-0.4}$ and $BNZFO_{-0.6}$ have bigger attenuation constant than the others, indicating better MA or attenuation. The comparing of the MA characteristics got in this research with those in other researches is shown in Fig. 8. It refers that the RL and efficient absorption bandwidth under −10 dB of this research are exceeding other researches. The high MA characteristic of this absorbing is referred to as its essential double normal resonance in microscale [113]. As well, the addition of 8th collection materials in SiCN ceramics [114–118], and other materials in SiC ceramics [119–121] can also promote the MA performance of absorbing to a big range.

These studies were shown the great effect of the change of method of preparation, the type of ferrite material, the effect of the process of substitution with different mineral cations, the thickness of the absorbent substances, and Doped on the microwave absorption properties. The microwave absorbing behavior of ferrite materials is shown in Table 2.

Table 2
Microwave absorbing behavior of ferrites and their composites.

Nanomaterial	T (mm)	Freq (GHz)	Max RL (dB)	$(B.W)_{-10\ dB}$ (GHz)	ε'_{max}	ε''_{max}	μ'_{max}	μ''_{max}	Refs.
Fe_3O_4 30 wt%	4.0	5.4	−26.9	3.1	9.3	0.3	1.2	0.52	[147]
Fe_3O_4 30 wt%	3.0	8.2	−21.1	2.7	9.5	0.4	0.9	0.38	
Fe_3O_4 40 wt%	3.0	6.9	−23.3	3.1	11.1	1.6	1.06	0.45	[148]
Fe_3O_4 40 wt%	3.5	5.5	−27.8	2.6	11.0	1.4	1.23	0.54	
Fe_3O_4 40 wt%	4.0	4.7	−44.7	2.1	11.0	1.3	1.30	0.58	
Fe_3O_4 nanowires	2.5	8.3	−16.7	2.7	6.2	0.2	0.98	0.20	[149]
Fe_3O_4 nanosheets	2.5	10.2	−8.89	0.0	8.1 2	2.1	0.90	0.01	
Fe_3O_4 90%	1.0	14.1	−42.3	4.3	23.6	2.9	0.3	0.3	[150]
Fe_3O_4 80%	1.3	15.1	−33.7	3.2	17.7	3.9	0.5	0.06	
Fe_3O_4 70%	5.0	3.4	−34.9	1.5	12.1	1.2	1.2	0.6	
Ni:B/Fe_3O_4	6.0	5.4	−28.4	2.6	6.6	1.0	0.8	0.3	[151]
$(Ni_{0.5}Zn_{0.5})Fe_2O_4$	2.97	11.9	−36.2	5.2	7.5	0.05	0.5	0.2	[152]
$(Ni_{0.4}Cu_{0.2}Zn_{0.4})Fe_2O_4$	9.2	1.1	−35.6	1.6	8.1	−0.01	2.1	3.8	
	4.2	4.1	−48.1	3.6	7.05	0.03	1.56	1.49	
$MnFe_2O_4$	2.0	9.4	−42.5	0.3	1.5	0.35	4.7	0.73	[153]
$Co_{0.5}Mn_{0.5}Fe_2O_4$	2.0	10.5	−47.0	1.0	3.8	0.36	7.1	1.02	
$CoFe_2O_4$	2.0	10.7	−39.8	1.0	7.5	0.46	8.9	1.42	
$Bi_{0.8}La_{0.2}FeO_3$	6.0	11.5	−29.7	1.1	9.8	1.4	1.0	0.9	[154]
PANI/$Li_{0.35}Zn_{0.3}Fe_{2.35}O_4$	2.0	14.6	−37.5	2.0	8.2	5.0	1.04	0.1	[155]
$Ni_{0.6}Zn_{0.4}Fe_2O_4$/PANI	2.6	12.8	−41.0	5.0	6.2	6.0	0.97	−0.05	[156]
C/Fe_3O_4	1.9	12.1	−52.8	2.5	12.0	1.5	0.94	0.10	[157]
C/Fe_3O_4 NR δ (0.5)	6.2	3.4	−55.7	2.9	11.5	2.7	1.35	0.54	[158]
C/Fe_3O_4 NR δ (1)	4.5	6.0	−55.1	2.8	10.6	2.5	0.88	0.26	
C/Fe_3O_4 NR δ (2)	4.2	6.1	−51.8	2.7	9.3	1.7	0.93	0.93	
C/Fe_3O_4 NR δ (4)	1.9	13.8	−55.3	3.8	6.7	1.6	0.95	−0.06	
ZnO/Fe_3O_4	5.0	1.66	−12.92	0.85	3.4	1.23	2.4	4.0	[159]
Fe:Mn/Fe_3O_4	1.85	13.9	−27.7	4.2	8.9	2.5	1.0	1.0	[160]
$(MnNi)_{0.2}Co_{0.6}BaTiFe_{10}O_{19}$	1.8	13.5	−53.0	5.4	6.7	0.4	0.8	0.7	[161]
$(MnNi)_{0.25}Co_{0.5}BaTiFe_{10}O_{19}$	1.8	14.1	−68.9	4.9	6.5	0.4	1.2	0.7	
ZnO/$BaFe_{12}O_{19}$	6.8	16.0	−37.3	3.0	3.1	1.3	0.7	0.03	[162]
$BaCe_{0.05}Fe_{11.95}O_{19}$	3.5	12.8	−37.4	8.1	2.72	1.38	1.10	0.38	[163]
	5.0	11.3	−31.5	3.5	1.6	1.6	1.4	0.77	
$ZnFe_2O_4$/rGO	2.5	9.3	−41.1	2.6	11.6	3.7	0.94	0.07	[164]
$NiFe_2O_4$/rGO	3.0	9.2	−39.6	3.0	8.0	3.0	1.0	0.1	[165]
	1.9	14.5	−36.9	5.2	9.0	1.6	0.78	0.2	
$CoFe_2O_4$/rGO	1.6	14.7	−44.1	4.5	9.4	9.3	0.98	0.5	[166]
$NiFe_2O_4$/grapheme/ polyaniline	2.5	12.5	−50.5	5.3	6.3	1.9	0.96	0.02	[167]
	3.0	10.0	−32.4	3.5	6.6	2.8	1.1	0.11	
MWCNT/$Ni_{0.5}Zn_{0.5}Fe_2O_4$	2	10.40	−10.03	0.08	18.5	8.5	0.98	0.03	[168]
	3	8.46	−19.34	1.24	11.7	4.2	0.94	0.01	
CF/Fe_3O_4/BN	3.0	12.5	−14.0	4.2	3.1	0.4	1.0	0.01	[169]

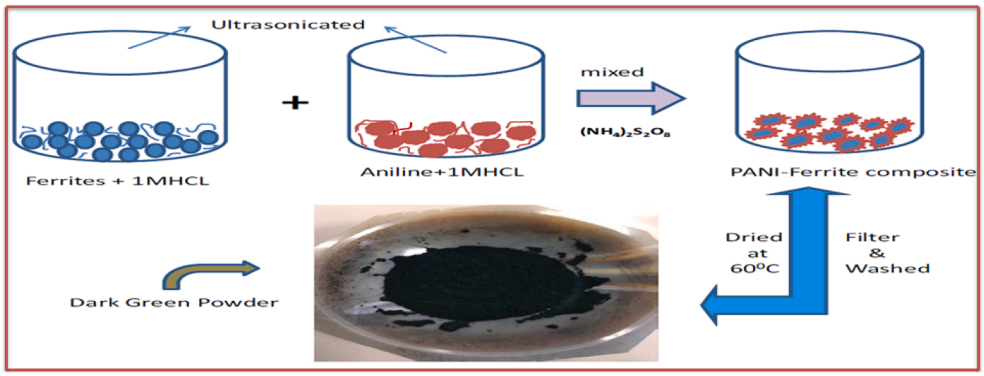

Fig 9. Polymerization technique of PANI–ferrite nanocomposite.

7. Microwave absorbent of ferrite/polymer composites:

The researchers attempted to improve the microwave absorption width by preparing composite materials with a microscopic structure (core/shell). The outer shell is formed from conductive polymers, while the inner core often is formed from ferrite material (spinel ferrite or hexagonal ferrite) [122,123]. Peng et al. prepared an absorbent composite material consisting of ferrite $Ni_{0.5x}Zn_{0.5x}Co_{2x}Fe_2O_4$ (x = 0–0.5) and thermoplastic polyurethane (TPU), with a Loading percentage of 80 wt% ferrite, where the highest absorption intensity was −20 dB at the frequency 5.14 GHz for the thickness of 5 mm, and the absorption bandwidth under −10 dB was 0.75 GHz [124]. Bhattacharyya et al. Prepared an absorbing nanocomposite by mixing the $Mg_{0.5}Zn_{0.5}Fe_2O_4$ with thermoplastic polyurethane at the frequency range (4–15 GHz), with a Loading percentage of 50 wt% ferrite, then applying the prepared mixture as a coating (thin layer 100 μm). This coating showed wide absorption with RL exceeding 88% of the incoming rays [125]. Furthermore, Singh et al. studied ternary core–shell $Mg_{0.6}Cu_{0.4}Fe_2O_4$ with PANI matrix nanocomposite by in-situ chemical polymerization technique as shown in Fig. 9, this lightweight nanocomposite displayed the important EM shielding impact of –32.8 dB in the frequency field of X-band [126]. Zhao et al. prepared PANI/$Co_{0.5}Zn_{0.5}Fe_2O_4$ by situ polymerization. The results illustrated that the maximum RL was −39.8 dB at the frequency of 22.3 GHz for the thickness of 2 mm, the absorption bandwidth under −10 dB was 10.5 GHz, the dielectric loss was (ε_r = 19.3- i13.1), and the magnetic loss was (μ_r = 1.7- i0.3) [127]. Dixit

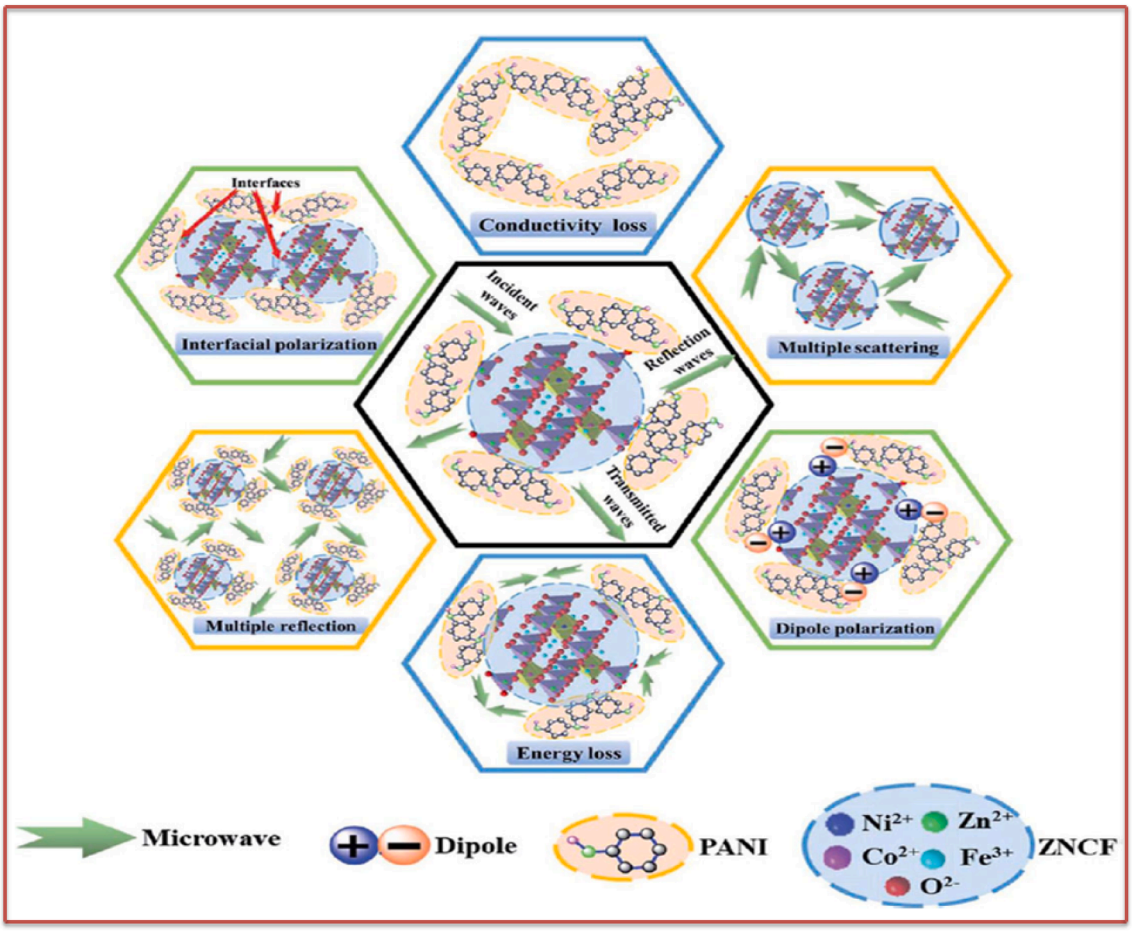

Fig 10. Schematic of MA mechanisms for the PANI/ZNCF compounds.

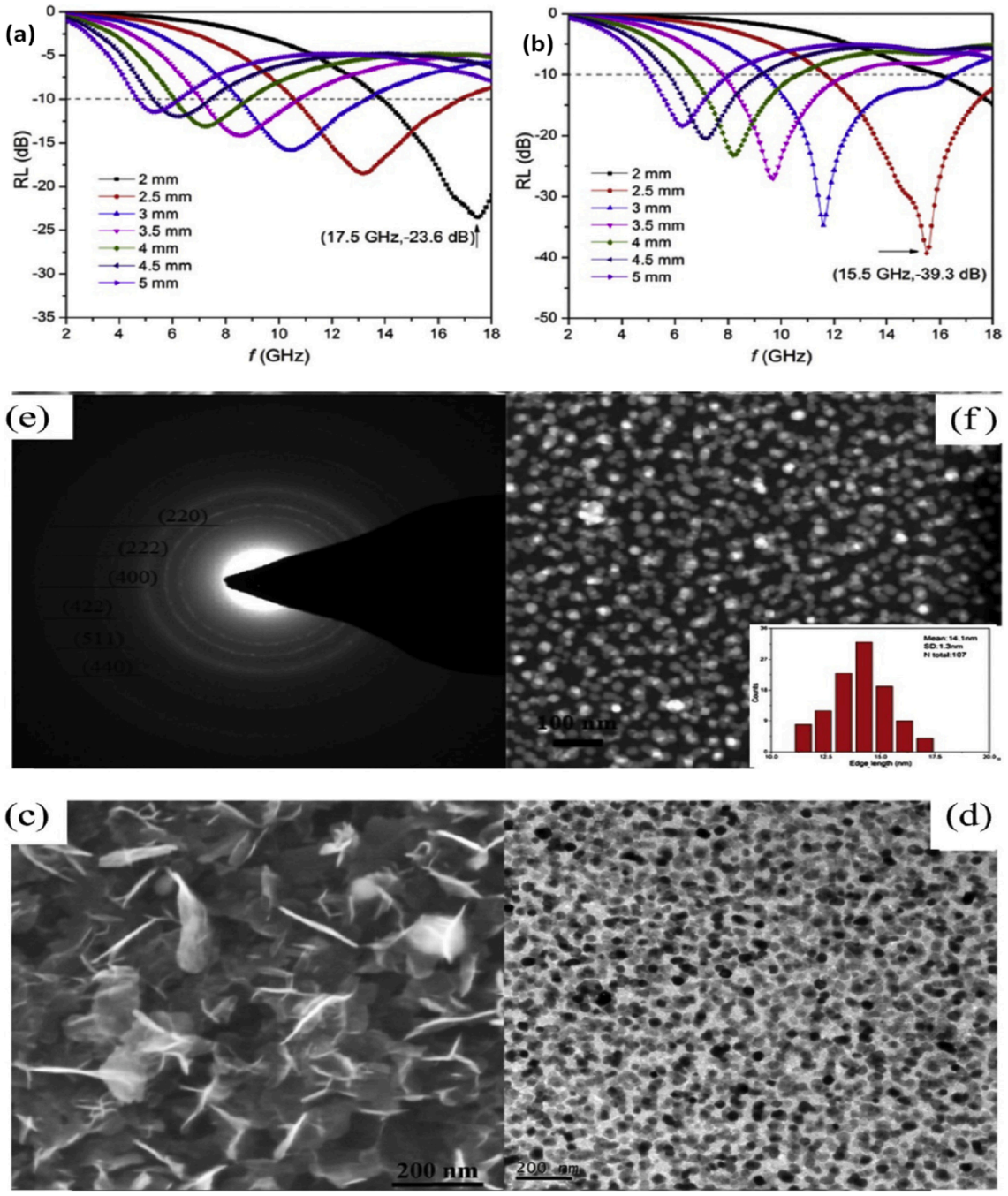

Fig 11. Calculated RL for (a) Amorphous carbon, (b) Fe_3O_4/C, and (c) SEM picture, (d) TEM picture, (e) SAED picture, and (f) HAADF picture for Fe_3O_4/C at a 1:1 ratio.

et al. prepared $BaCo_{0.9}Fe_{0.05}Si_{0.95}Fe_{10.1}O_{19}$ was dispersed in a polyurethane matrix according to the loading percentages (50, 60, 70, 80%). The composite material with a loading ratio of 80 wt% ferrite showed the highest absorption intensity was −24.5 dB at the frequency of 12 GHz for the thickness of 1.6 mm, and the absorption bandwidth under −10 dB was 2 GHz [128].

On the other hand, other researchers have studied the core/shell/shell on microwave absorption properties. Zhai et al. prepared Fe_3O_4@SiO_2@PPy (core/shell/shell) via microemulsion polymerization technique. The highest absorption intensity was −40.9 dB at the frequency of 6 GHz for the thickness of 5 mm, and the absorption bandwidth under −10 dB was 6.88 GHz [129]. Weng et al. were able to prepare the composite material Fe_3O_4/ polyaniline/Polypyrrole that exceeded the −10 dB threshold across the entire frequency range (X-band), 5.4 GHz within (Ku-band), and 1.3 GHz within (C-band) for the thickness of 2.6 mm and a loading percentage of 20% $_{w/w}$. As well, the combination of polymer with ion-doped ferrites is also an efficient approach to get EM absorbers with excellent behavior [130]. Yao et al. explained the systematic impact of interaction circumstances on the characteristics of Co-doped Zn-Ni ferrite/PANI hybrids prepared through interfacial polymerization. The realization outcomes refer that the hybrid gives premium EM absorbing characteristics with maximum RL value of −54.3 dB and efficient absorbing bandwidth under −10 dB was 6.02 GHz for the thickness of 6.8 mm in the optimized polymerization circumstances of 20 °C for 12 h. The outstanding EM absorbing characteristics of this PANI/Zn-Ni ferrite hybrid can be illustrated in

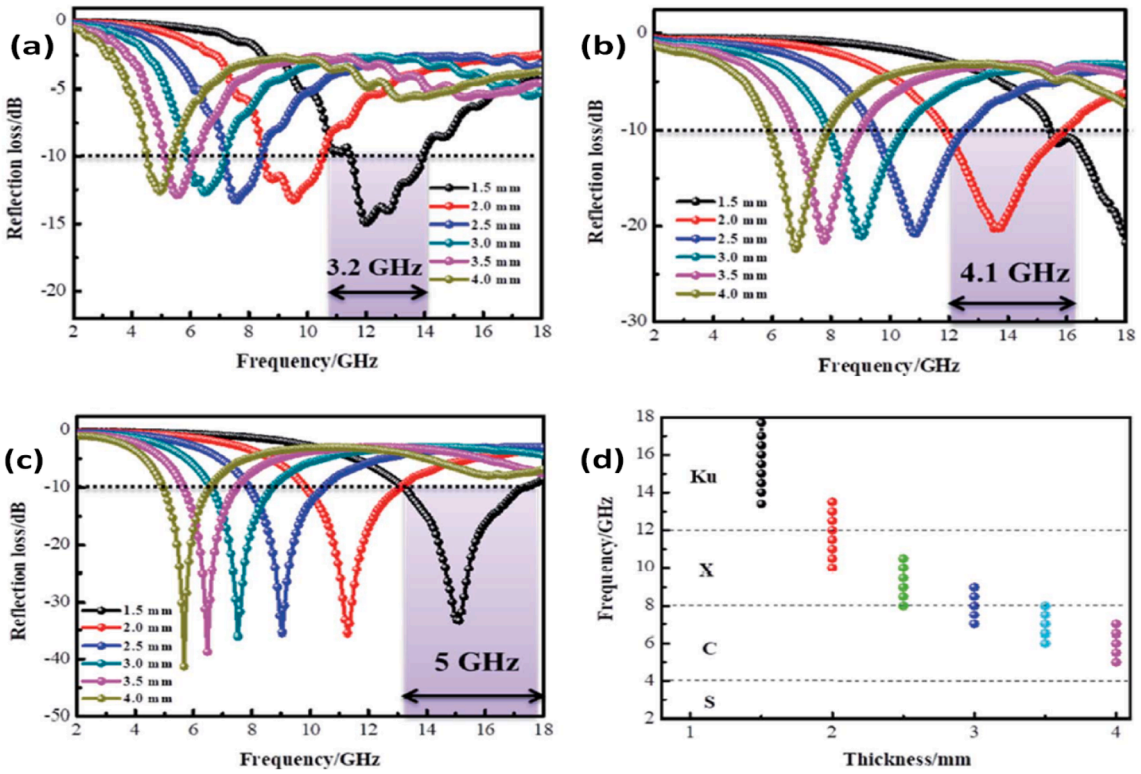

Fig 12. RL curves of CF (a), CF@$CoFe_2O_4$ (b) and CF@$CoFe_2O_4$@MnO_2 composites (c) Efficient absorption bandwidth of CF@$CoFe_2O_4$@MnO_2 composite at a various thicknesses (d).

Fig. 10 for the perfect impedance matching properties, powerful dipole polarization and interfacial polarization impact marked conductivity loss, and multiple dissipation and reflection [131]. On the other hand, in several states, the polymer-based ferrite compounds can be inserted with carbon substances also, e.g. core–shell ferrite/graphene oxide/polyaniline [15], Fe_3O_4@C@PANI [132], cobalt ferrite/graphene/polyaniline [133], and so on. These compounds can own unique EM absorption performance because of the connection absorbing mechanism to present in every part. The review of these researches we were shown illustrates the capacity of these composites to the microwave absorption better compared to ferrite materials and which are characterized by their lightweight and relatively low thickness. The microwave absorbing behavior of ferrite polymer composites is shown in Table 2.

8. Microwave absorbent of ferrite/carbon composites

The nanostructured carbon materials have unique properties, like high conductivity, control of porosity, high mechanical strength, and superb physicochemical characteristics due to their nanoscale size, and the ratio of surface area to volume is quite aloft [134,135]. These prominent structural properties of carbon nanomaterials assist them in reacting with other substances for many new applications, like microwave absorption, and bio, chemical, and mechanical sensors. Many researchers studied the effect of adding different types of carbon (eg, carbon nanotubes (CNTs), carbon fibers (CF), graphene, etc) to ferrite magnetic materials on the microwave absorption that aims to obtain wide absorption bandwidth or reduce both the thickness and the loading percentage. Ahmad et al. prepared a composite material of Ni-Zn ferrite and carbon nanotube through physical mixing. They studied the microwave absorption of the prepared material with a loading percentage of 2.0%$_{w/w}$ for the thickness of 1.0 mm. This material managed to exceed the absorption threshold −10 dB within the two ranges (8.0–12.5 GHz) and (1.0–8.0 GHz) with values of 3.7 GHz and 0.9 GHz, respectively [136]. On the other hand, a number of researchers have studied the addition of amorphous carbon to Fe_3O_4, for example, Liu et al. prepared amorphous carbon and Fe_3O_4/C, the results for amorphous carbon were showed for RL was –23.6 dB for the thickness of 2 mm at the frequency of 17.5 GHz, the dielectric loss was (ε_r = 5.1- i3.2), and the magnetic loss was (μ_r = 1.01 + i0.019). As for Fe_3O_4/C, the results illustrated RL was −39.3 dB for the thickness of 2.5 mm at the frequency of 15.5 GHz for a 1:1 loading percentage by weight, the dielectric loss was (ε_r = 4.5- i2.5), and the magnetic loss was (μ_r = 1.04 + i0.019). Fig. 11 shows the outcomes were compared between amorphous carbon and Fe_3O_4/C at different thicknesses and implemented some experimental analyses for Fe_3O_4/C at a 1:1 ratio [137]. Besides, a number of researchers have analyzed the effect of carbon concentration on Fe_3O_4, for instance, Wang et al. prepared Fe_3O_4@C (17.84 wt%C), and Fe_3O_4@C (23.41 wt%C) prepared through in-situ polymerization. The results illustrated for Fe_3O_4@C (17.84 wt%C) that the RL was −35.8 dB at the frequency of 4.7 GHz for the thickness of 5 mm, the absorption bandwidth under −10 dB was 1.7 GHz, the dielectric loss was (ε_r = 9.4- i2.9), and the magnetic loss was (μ_r = 1.1- i0.2). As for Fe_3O_4@C (23.41 wt%C) that the RL was −40.2 dB for the thickness of 1.5 mm at the frequency 15.8 GHz, the absorption bandwidth under −10 dB was 3.9 GHz, the dielectric loss is (ε_r = 10.2- i3.7), and the magnetic loss is (μ_r = 1) [138]. In other cases, a number of researchers have investigated the effect of carbon fiber on ferrite, for instance, Feng et al. prepared CF@$CoFe_2O_4$ and CF@$CoFe_2O_4$@MnO_2 composites by the sol–gel technique and hydrothermal interaction. The as-synthesized CF@$CoFe_2O_4$@MnO_2 composite showed superior MA performance fundamentally because of reasonable EM matching, and its minimum RL value equaled −34 dB with a pattern thickness of 1.5 mm. Fig. 12 shows RL curves of CF (a), CF@$CoFe_2O_4$ (b) and CF@$CoFe_2O_4$@MnO_2 composites (c) at a various thicknesses the efficient absorption bandwidth of CF@$CoFe_2O_4$@MnO_2 composite (d) [139].

On the other hand, a number of researchers have studied the addition of graphene to ferrite, for example, Huang et al. prepared $NiFe_2O_4$ with garnished graphene (GR) as the substrate for the immediate growth of

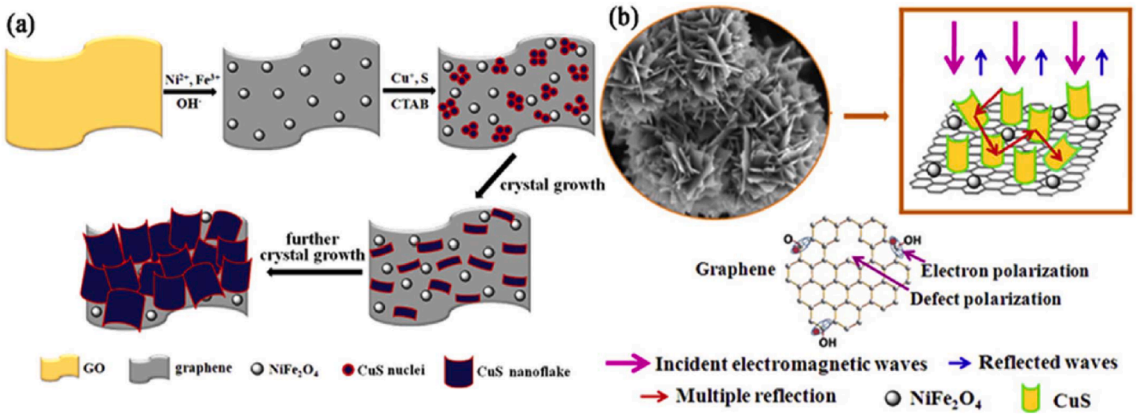

Fig 13. (a) Explanation for the shaping of magnetically garnished GR@CuS. (b) Prospective the mechanism of MA in magnetically garnished GR@CuS.

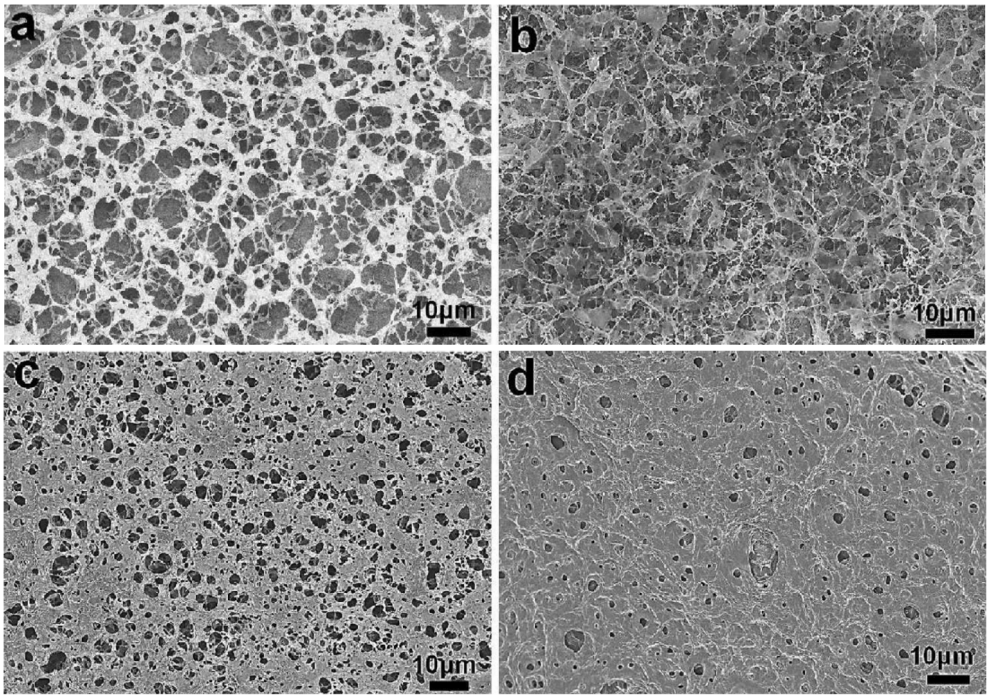

Fig 14. Illustration of the manufactured microstructure of interconnected network made of rGO and CNTs with Fe_3O_4 magnetic particles.

CuS nanoflakes by the hydrothermal process in alkaline conditions. Fig. 13(a) shows the shaping operation of magnetically garnished GR@CuS. The results illustrated the RL was −54.5 dB for the thickness of 2.5 mm at the frequency of 11.4 GHz, and the absorption bandwidth under −10 dB was 4.5 GHz. Fig. 13(b) shows the mechanism of MA, the entering of magnetic particles in GR sheets, and CuS nanoflakes worked as a significant factor in improving the microwave absorption characteristics [140].

In other cases, a number of researchers have investigated the effect of reduced graphene oxide (rGO) on ferrite, for instance, Zhang et al. prepared $CoFe_2O_4$:SnS_2/rGO composite by hydrothermal technique. The results illustrated that the RL was −54.4 dB at the frequency 16.5 GHz for the thickness of 1.6 mm, the absorption bandwidth under −10 dB was 12 GHz, the dielectric loss was (ε_r = 7.3- i2.7), and the magnetic loss was (μ_r = 1- i0.1) [141]. Huang et al. prepared RGO/$CoFe_2O_4$ composite by hydrothermal technique. The results illustrated that the RL was −37.2 dB at the frequency 11.6 GHz for the thickness of 2.5 mm, the absorption bandwidth under −10 dB was 4.2 GHz, the dielectric loss was (ε_r = 7.1- i2.8), and the magnetic loss was (μ_r = 1- i0.1) [142]. Yunzhu et al. collected 3D network layers of reduced graphene oxide on the surface of carbon nanotube/ Fe_3O_4 films by using an electrophoretic method. The results illustrated that the high absorption intensity for this composite was −50.5 dB at the thickness of 1.42 mm with the absorption bandwidth under −10 dB is 5.7 GHz. Fig. 14 illustrated that the manufactured microstructure of the interconnected network was made of reduced graphene oxide and carbon nanotubes with Fe_3O_4 magnetic particles [143]. Accordingly, it appeared that the graphene has elevated special surface areas that were so fit for loading ferrite nanoparticles [144–146]. Consequently like this hybrid is a unique candidate for utilization as the microwave absorber.

The summary of these studies which we were shown illustrates the ability of these composites to the microwave absorption, as these composites were distinguished as having wide bandwidth and lightweight with thin thickness. Table 2 is shown the microwave absorbing behavior of absorbent ferrite/carbon.

9. Summary and conclusions

The current review includes a discussion about the reflection loss mechanism which is due to firstly the dielectric loss mechanism which happens basically from conduction loss and polarization relaxations. Secondly, the magnetic loss mechanism which happens basically from natural resonance, domain wall resonance, and eddy current effect. In order to obtain efficient EM wave absorption materials, there should be efficient integration between dielectric and magnetic losses, so that to meet the requirement of the impedance matching condition along with the high absorption properties of the materials. Furthermore, the properties of hexagonal ferrites and spinel ferrites were highlighted. Hexagonal ferrites have a high crystalline magnetic field and that enhances their normal resonance in the upper GHz band, whereas the spinel ferrites have a low crystalline magnetic field and are used in microwave absorption applications that have a low resonance frequency. Also, the synthesis techniques of nano ferrites were highlighted and the advantages and disadvantages of each synthesis technique were pointed outs. The data analysis indicates that the shape and size of various nanomaterials are directly related to the preparation method. Furthermore, the microwave absorption performances of nano ferrites are organized according to different parameters like precursor composition, combustion temperature, pH of the solution, etc. The current collection of scientific literature involves various groups of nano ferrites that interact with incident EM radiation in various models. The shape of the nano ferrites reaction with EM radiation is determined by the permeability and permittivity of a prepared substance. The researchers can estimate the RL of nano ferrites using complex permeability and permittivity related to substance thickness and frequency. Studies have shown that changing crystal structure, particle morphology, and a composite percentage will impact reflection loss value, and as well as absorption bandwidth. On the other hand, the results have shown the far better performance of composite materials with a nano ferrite core and a conducting polymer shell and composite materials (ferrite/carbon) than microwave absorbers of nano ferrite materials which are characterized by their lightweight and relatively low thickness. Eventually, understanding how to fabricate these materials is primary to control the characteristics of the final microwave absorber according to its potential applications.

Declaration of Competing Interest

The authors declare that they have no known competing financial interests or personal relationships that could have appeared to influence the work reported in this paper.

References:

[1] H. Lv, Z. Yang, S.J.H. Ong, C. Wei, H. Liao, S. Xi, Y. Du, G. Ji, Z.J. Xu, A Flexible Microwave Shield with Tunable Frequency-Transmission and Electromagnetic Compatibility, Adv. Funct. Mater. 29 (14) (2019) 1900163, https://doi.org/10.1002/adfm.v29.1410.1002/adfm.201900163.

[2] C. Liang, H. Qiu, P. Song, X. Shi, J. Kong, J. Gu, Ultra-light MXene aerogel/wood-derived porous carbon composites with wall-like "mortar/brick" structures for electromagnetic interference shielding, Sci. Bull. 65 (8) (2020) 616–622, https://doi.org/10.1016/j.scib.2020.02.009.

[3] X. Chen, T. Shi, K. Zhong, G. Wu, Y. Lu, Capacitive behavior of MoS2 decorated with FeS2@carbon nanospheres, Chem. Eng. J. 379 (2020) 122240, https://doi.org/10.1016/j.cej.2019.122240.

[4] S. Chen, G. Meng, B.o. Kong, B. Xiao, Z. Wang, Z. Jing, Y. Gao, G. Wu, H. Wang, Y. Cheng, Asymmetric alicyclic amine-polyether amine molecular chain structure for improved energy storage density of high-temperature crosslinked polymer capacitor, Chem. Eng. J. 387 (2020) 123662, https://doi.org/10.1016/j.cej.2019.123662.

[5] C. Cheng, Z. Chen, Z. Huang, C. Zhang, R. Tusiime, J. Zhou, Z. Sun, Y. Liu, M. Yu, H. Zhang, Simultaneously improving mode I and mode II fracture toughness of the carbon fiber/epoxy composite laminates via interleaved with uniformly aligned PES fiber webs, Compos. Part A Appl. Sci. Manuf. 129 (2020) 105696, https://doi.org/10.1016/j.compositesa:2019.105696.

[6] H. Xu, X. Yin, X. Li, M. Li, S. Liang, L. Zhang, L. Cheng, Lightweight Ti 2 CT x MXene/Poly(vinyl alcohol) Composite Foams for Electromagnetic Wave Shielding with Absorption-Dominated Feature, ACS Appl. Mater. Interfaces. 11 (10) (2019) 10198–10207, https://doi.org/10.1021/acsami.8b2167110.1021/acsami.8b21671.s001.

[7] L.d.C. Folgueras, M.C. Rezende, Multilayer radar absorbing material processing by using polymeric nonwoven and conducting polymer, Mater. Res. 11 (3) (2008) 245–249, https://doi.org/10.1590/S1516-14392008000300003.

[8] L.C. Folgueras, M.A. Alves, M.C. Rezende, Evaluation of a nanostructured microwave absorbent coating applied to a glass fiber/polyphenylene sulfide laminated composite, Mater. Res. 17 (2014) 197–202, https://doi.org/10.1590/S1516-14392014005000009.

[9] Y. Liu, X. Liu, X. Wang, Synthesis and microwave absorption properties of Ni-Zn-Mn spinel ferrites, Adv. Appl. Ceram. 114 (2) (2015) 82–86, https://doi.org/10.1179/1743676114Y.0000000194.

[10] W. Ari Adi, Y. Yunasfi, M. Mashadi, D. Sahidin Winatapura, A. Mulyawan, Y. Sarwanto, Y. Edi Gunanto, Y. Taryana, Metamaterial: Smart Magnetic Material for Microwave Absorbing Material, Electromagn. Fields Waves. (2019) 1–18, https://doi.org/10.5772/intechopen.84471.

[11] P.-J. Liu, Z.-J. Yao, V.M.H. Ng, J.-T. Zhou, Z.-H. Yang, L.-B. Kong, Enhanced microwave absorption properties of double-layer absorbers based on spherical NiO and Co0.2Ni0.4Zn0.4Fe2O4 ferrite composites, Acta Metall. Sin. (English Lett. 31 (2) (2018) 171–179, https://doi.org/10.1007/s40195-017-0612-5.

[12] T. Indrusiak, I.M. Pereira, A.P. Heitmann, J.G. Silva, Â.M.L. Denadai, B.G. Soares, Epoxy/ferrite nanocomposites as microwave absorber materials: effect of multilayered structure, J. Mater. Sci. Mater. Electron. 31 (16) (2020) 13118–13130, https://doi.org/10.1007/s10854-020-03863-0.

[13] W. Jang, S. Mallesh, S.B. Lee, K.H. Kim, Microwave absorption properties of core-shell structured FeCoNi@PMMA filled in composites, Curr. Appl. Phys. 20 (4) (2020) 525–530, https://doi.org/10.1016/j.cap.2020.01.019.

[14] Z. Du, Y. Zhang, X. Chen, X. Que, P. Liu, M. Zhai, H.-L. Ma, X. Zhang, Radiation-induced synthesis of graphene/ferrites nanocomposites for enhanced microwave-absorbing properties, J. Mater. Sci. Mater. Electron. 31 (19) (2020) 16281–16289, https://doi.org/10.1007/s10854-020-04176-y.

[15] J. Sun, L. Wang, Q. Yang, Y. Shen, X. Zhang, Preparation of copper-cobalt-nickel ferrite/graphene oxide/polyaniline composite and its applications in microwave absorption coating, Prog. Org. Coatings. 141 (2020) 105552, https://doi.org/10.1016/j.porgcoat.2020.105552.

[16] M. Green, Y. Li, Z. Peng, X. Chen, Dielectric, magnetic, and microwave absorption properties of polyoxometalate-based materials, J. Magn. Magn. Mater. 497 (2020) 165974, https://doi.org/10.1016/j.jmmm.2019.165974.

[17] V. Pratap, B. Singh, S. Kumar, A.K. Soni, M. Katiyar, Electromagnetic and microwave absorbing properties of U-type barium hexaferrite / polyaniline-epoxy composites Electromagnetic and Microwave Absorbing Properties of U- type Barium Hexaferrite / Polyaniline-Epoxy, Composites 080003 (2020) 1–6.

[18] S. Du, H. Chen, R. Hong, Preparation and electromagnetic properties characterization of reduced graphene oxide/strontium hexaferrite nanocomposites, Nanotechnol. Rev. 9 (2020) 105–114, https://doi.org/10.1515/ntrev-2020-0010.

[19] F. Qin, C. Brosseau, A review and analysis of microwave absorption in polymer composites filled with carbonaceous particles, J. Appl. Phys. 111 (6) (2012) 061301, https://doi.org/10.1063/1.3688435.

[20] E. Michielssen, J.M. Sajer, R. Mittra, Pareto-optimal design of broadband microwave absorbers using genetic algorithms, AP-S Int, Symp. (IEEE Antennas Propag. Soc. 3 (1993) 1167–1170, https://doi.org/10.1109/aps.1993.385141.

[21] H. Hosseini, H. Mahdavi, Nanocomposite based on epoxy and MWCNTs modified with NiFe2O4 nanoparticles as efficient microwave absorbing material, Appl. Organomet. Chem. 32 (4) (2018) e4294, https://doi.org/10.1002/aoc.v32.410.1002/aoc.4294.

[22] M. Sharma, D. Singh, A. Menon, G. Madras, S. Bose, Suppressing electromagnetic radiation by trapping ferrite nanoparticles and carbon nanotubes in hierarchical nanoporous structures designed by crystallization-induced phase separation, ChemistrySelect. 3 (4) (2018) 1189–1201, https://doi.org/10.1002/slct.201702731.

[23] Q. Zhang, Z. Du, X. Huang, Z. Zhao, T. Guo, G. Zeng, Y. Yu, Tunable microwave absorptivity in reduced graphene oxide functionalized with Fe 3 O 4 nanorods, Appl. Surf. Sci. 473 (2019) 706–714, https://doi.org/10.1016/j.apsusc.2018.12.130.

[24] N. Li, G. Huang, H. Xiao, Q. Feng, S. Fu, Investigations on structure-dependent microwave absorption performance of nano-Fe 3 O 4 coated carbon-based absorbers, Carbon N. Y. 144 (2019) 216–227, https://doi.org/10.1016/j.carbon.2018.12.036.

[25] P. Xie, Y. Li, Q. Hou, K. Sui, C. Liu, X. Fu, J. Zhang, V. Murugadoss, J. Fan, Y. Wang, R. Fan, Z. Guo, Tunneling-induced negative permittivity in Ni/MnO nanocomposites by a bio-gel derived strategy, J. Mater. Chem. C. 8 (9) (2020) 3029–3039, https://doi.org/10.1039/C9TC06378A.

[26] M. Gao, Y. Zhao, S. Wang, Y. Xu, C. Feng, D. Shi, Q. Jiao, Preparation of pod-like 3D Ni 0.33 Co 0.67 Fe 2 O 4 @rGO composites and their microwave absorbing properties, Ceram. Int. 45 (6) (2019) 7188–7195, https://doi.org/10.1016/j.ceramint.2018.12.226.

[27] P. Gairola, S.P. Gairola, S.K. Dhawan, R.P. Tandon, V. Gupta, L.P. Purohit, S. Sharma, Carbon material-nanoferrite composite for radiation shielding in microwave frequency, Integr. Ferroelectr. 186 (1) (2018) 40–48, https://doi.org/10.1080/10584587.2017.1369324.

[28] Z.-J. Guan, J.-T. Jiang, N.a. Chen, Y.-X. Gong, L. Zhen, Carbon-coated CoFe-CoFe2O4 composite particles with high and dual-band electromagnetic wave absorbing properties, Nanotechnology. 29 (30) (2018) 305604, https://doi.org/10.1088/1361-6528/aac31f.

[29] S. Gao, Q. Wang, Y. Lin, H. Yang, L. Wang, Flower-like Bi0.9La0.1FeO3 microspheres modified by reduced graphene oxide as a thin and strong electromagnetic wave absorber, J. Alloys Compd. 781 (2019) 723–733, https://doi.org/10.1016/j.jallcom.2018.11.327.

[30] B. Qu, H. Du, Z. Yang, Lead-free relaxor ferroelectric ceramics with high optical transparency and energy storage ability, J. Mater. Chem. C. 4 (9) (2016) 1795–1803, https://doi.org/10.1039/C5TC04005A.

[31] G. Wu, Y.u. He, H. Zhan, Q.Q. Shi, J.N. Wang, A novel Fe3O4/carbon nanotube composite film with a cratered surface structure for effective microwave absorption, J. Mater. Sci. Mater. Electron. 31 (14) (2020) 11508–11519, https://doi.org/10.1007/s10854-020-03698-9.

[32] A.A. Birajdar, A. A. Birajdar (2010) 1–19.

[33] S.F. Mansour, O.M. Hemeda, M.A. Abdo, W.A. Nada, Improvement on the magnetic and dielectric behavior of hard/soft ferrite nanocomposites, J. Mol. Struct. 1152 (2018) 207–214, https://doi.org/10.1016/j.molstruc.2017.09.089.

[34] W. Solano-Alvarez, E.J. Pickering, M.J. Peet, K.L. Moore, J. Jaiswal, A. Bevan, H. K.D.H. Bhadeshia, Soft novel form of white-etching matter and ductile failure of carbide-free bainitic steels under rolling contact stresses, Acta Mater. 121 (2016) 215–226, https://doi.org/10.1016/j.actamat.2016.09.012.

[35] N. Modaresi, R. Afzalzadeh, B. Aslibeiki, P. Kameli, A. Ghotbi Varzaneh, I. Orue, V.A. Chernenko, Magnetic properties of Zn x Fe 3–x O 4 nanoparticles: A competition between the effects of size and Zn doping level, J. Magn. Magn. Mater. 482 (2019) 206–218, https://doi.org/10.1016/j.jmmm.2019.03.060.

[36] A. Namai, M. Yoshikiyo, K. Yamada, S. Sakurai, T. Goto, T. Yoshida, T. Miyazaki, M. Nakajima, T. Suemoto, H. Tokoro, S.I. Ohkoshi, Hard magnetic ferrite with a gigantic coercivity and high frequency millimetre wave rotation, Nat. Commun. 3 (2012) 1035–1036, https://doi.org/10.1038/ncomms2038.

[37] K.S. Martirosyan, N.S. Martirosyan, A.E. Chalykh, Structure and properties of hard-magnetic barium, strontium, and lead ferrites, Inorg. Mater. 39 (2003) 866–870, https://doi.org/10.1023/A:1025037716108.

[38] S. Torkian, A. Ghasemi, R.S. Razavi, Magnetic properties of hard-soft SrFe10Al2O19/Co0.8Ni0.2Fe2O4 ferrite synthesized by one-pot sol-gel auto-combustion, J. Magn. Magn. Mater. 416 (2016) 408–416, https://doi.org/10.1016/j.jmmm.2016.05.050.

[39] F.J. Heiligtag, M. Niederberger, The fascinating world of nanoparticle research, Mater. Today. 16 (7-8) (2013) 262–271, https://doi.org/10.1016/j.mattod.2013.07.004.

[40] S. He, H. Zhang, Y. Liu, F. Sun, X. Yu, X. Li, L.i. Zhang, L. Wang, K. Mao, G. Wang, Y. Lin, Z. Han, R. Sabirianov, H. Zeng, Maximizing Specific Loss Power for Magnetic Hyperthermia by Hard-Soft Mixed Ferrites, Small. 14 (29) (2018) 1800135, https://doi.org/10.1002/smll.v14.2910.1002/smll.201800135.

[41] A. Hajalilou, S.A. Mazlan, A review on preparation techniques for synthesis of nanocrystalline soft magnetic ferrites and investigation on the effects of microstructure features on magnetic properties, Appl. Phys. A Mater. Sci. Process. 122 (7) (2016), https://doi.org/10.1007/s00339-016-0217-2.

[42] H. Zhao, C. Ragusa, C. Appino, O. de la Barriere, Y. Wang, F. Fiorillo, Energy Losses in Soft Magnetic Materials under Symmetric and Asymmetric Induction Waveforms, IEEE Trans. Power Electron. 34 (3) (2019) 2655–2665, https://doi.org/10.1109/TPEL.2018.2837657.

[43] J. Füzer, M. Strečková, S. Dobák, Ľ. Ďáková, P. Kollár, M. Fáberová, R. Bureš, Y. Osadchuk, P. Kurek, M. Vojtko, Innovative ferrite nanofibres reinforced soft magnetic composite with enhanced electrical resistivity, J. Alloys Compd. 753 (2018) 219–227, https://doi.org/10.1016/j.jallcom.2018.04.237.

[44] V.S. Coker, N.D. Telling, G. van der Laan, R.A.D. Pattrick, C.I. Pearce, E. Arenholz, F. Tuna, R.E.P. Winpenny, J.R. Lloyd, Harnessing the extracellular bacterial production of nanoscale cobalt ferrite with exploitable magnetic properties, ACS Nano. 3 (7) (2009) 1922–1928, https://doi.org/10.1021/nn900293d.

[45] K. Pubby, K. Vijay Babu, S. Bindra Narang, Magnetic, elastic, dielectric, microwave absorption and optical characterization of cobalt-substituted nickel spinel ferrites, Mater. Sci. Eng. B Solid-State Mater. Adv. Technol. 255 (2020) 114513, https://doi.org/10.1016/j.mseb.2020.114513.

[46] L. Kerkeni, P. Ruano, L.L. Delgado, S. Picco, L. Villegas, F. Tonelli, M. Merlo, J. Rigau, D. Diaz, M. Masuelli, We are IntechOpen, the world ' s leading publisher of Open Access books Built by scientists, for scientists TOP 1 %, Intech. (2016) 13.

[47] M.N. Akhtar, M. Saleem, M.A. Khan, Al doped spinel and garnet nanostructured ferrites for microwave frequency C and X- band applications, J. Phys. Chem. Solids. 123 (2018) 260–265, https://doi.org/10.1016/j.jpcs.2018.08.007.

[48] S. Kumar, D.P. Dubey, S. Shannigrahi, R. Chatterjee, Complex permittivity, permeability, magnetic and microwave absorbing properties of Ni2+ substituted mechanically milled U-type hexaferrites, J. Alloys Compd. 774 (2019) 52–60, https://doi.org/10.1016/j.jallcom.2018.09.339.

[49] Y. Song, J.i. Zheng, M. Sun, S. Zhao, The electromagnetic and microwave absorbing properties of polycrystalline Y-type Ba1.5Sr0.5CoZnFe12−xAlxO22 hexaferrites over the microwave range, J. Mater. Sci. Mater. Electron. 27 (4) (2016) 4131–4138, https://doi.org/10.1007/s10854-016-4272-4.

[50] A.R. Farhadizadeh, S.A. Seyyed Ebrahimi, S.M. Masoudpanah, Effect of Nd3+ Substitution on the Phase Evolution and Magnetic Properties of W-Type Strontium Hexaferrite, J. Supercond. Nov. Magn. 29 (5) (2016) 1273–1278, https://doi.org/10.1007/s10948-016-3402-9.

[51] G.R. Gordani, M. Mohseni, A. Ghasemi, S.R. Hosseini, Microstructure, magnetic and microwave absorptive behavior of doped W-type hexaferrite nanoparticles prepared by co-precipitation method, Mater. Res. Bull. 76 (2016) 187–194, https://doi.org/10.1016/j.materresbull.2015.12.021.

[52] I. Sadiq, F. Sadiq, A. Shahzad, A. Sadiq, H.M. Khan, S. Naseem, S. Riaz, Theoretical and Experimental Investigation of Microwave Absorbing X-Type Hexaferrites Nanomaterial Synthesized by Cotton Soaked Method, IEEE Trans. Magn. 56 (8) (2020) 1–10, https://doi.org/10.1109/TMAG.2010.1109/TMAG.2020.3001442.

[53] D. Guo, W. Kong, J. Feng, X. Li, X. Fan, Microwave absorption properties of SrxBa3-xCo2Fe24O41 hexaferrites in the range of 0.1–18 GHz, J. Alloys Compd. 751 (2018) 80–85, https://doi.org/10.1016/j.jallcom.2018.04.107.

[54] R. Padmanaban K. Venkatramanan S. Girivel K. Kasthuri A. Usharani A. Gayathri R. Vellaichamy Recent Trends in Materials Science (RTMS-2011), Recent Trends Mater. Sci. Appl. (2017) 2011. 10.1007/978-3-319-44890-9.

[55] Z. Ding, W. Wang, S. Wu, J.P. Liu, Synthesis and Characterization of Co-Zn Ferrite Nanoparticles by Hydrothermal Method: A Comparative Study, IEEE Trans. Magn. 51 (11) (2015) 1–4, https://doi.org/10.1109/TMAG.2015.2437895.

[56] I. Zalite, G. Heidemane, L. Kuznetsova, M. Maiorov, Hydrothermal synthesis of cobalt ferrite nanosized powders, IOP Conf. Ser. Mater. Sci. Eng. 77 (2015) 012011, https://doi.org/10.1088/1757-899X/77/1/012011.

[57] K. Praveena, K. Sadhana, H.L. Liu, M. Bououdina, Microwave absorption studies of magnetic sublattices in microwave sintered Cr3+ doped SrFe12O19, J. Magn. Magn. Mater. 426 (2017) 604–614, https://doi.org/10.1016/j.jmmm.2016.11.013.

[58] G. Biasotto, A.Z. Simões, C.R. Foschini, M.A. Zaghete, J.A. Varela, E. Longo, Microwave-hydrothermal synthesis of perovskite bismuth ferrite nanoparticles, Mater. Res. Bull. 46 (12) (2011) 2543–2547, https://doi.org/10.1016/j.materresbull.2011.08.010.

[59] S. Mallesh, A. Sunny, M. Vasundhara, V. Srinivas, Structure and magnetic properties of ZnO coated MnZn ferrite nanoparticles, J. Magn. Magn. Mater. 418 (2016) 112–117, https://doi.org/10.1016/j.jmmm.2016.03.017.

[60] P.Y. Jia, X.M. Liu, G.Z. Li, M. Yu, J. Fang, J. Lin, Sol-gel synthesis and characterization of SiO2@CaWO 4, SiO2@CaWO4:Eu3+/Tb3+ core-shell structured spherical particles, Nanotechnology. 17 (3) (2006) 734–742, https://doi.org/10.1088/0957-4484/17/3/020.

[61] N.H. Sulaiman, M.J. Ghazali, B.Y. Majlis, J. Yunas, M. Razali, F. Liu, D.-H. Lee, R. Lagoa, S. Kumar, Superparamagnetic calcium ferrite nanoparticles synthesized using a simple solgel method for targeted drug delivery, Biomed. Mater. Eng. 26 (s1) (2015) S103–S110, https://doi.org/10.3233/BME-151295.

[62] S. Mallesh, V. Srinivas, M. Vasundhara, K.H. Kim, Low-temperature magnetization behaviors of superparamagnetic MnZn ferrites nanoparticles, Phys. B Condens. Matter. 582 (2020) 411963, https://doi.org/10.1016/j.physb:2019.411963.

[63] R. Dehghan, S.A. Seyyed Ebrahimi, A. Badiei, Investigation of the effective parameters on the synthesis of Ni-ferrite nanocrystalline powders by coprecipitation method, J. Non. Cryst. Solids. 354 (47-51) (2008) 5186–5188, https://doi.org/10.1016/j.jnoncrysol.2008.08.015.

[64] P.P. Hankare, S.D. Jadhav, U.B. Sankpal, S.S. Chavan, K.J. Waghmare, B. K. Chougule, Synthesis, characterization and effect of sintering temperature on magnetic properties of MgNi ferrite prepared by co-precipitation method, J. Alloys Compd. 475 (1-2) (2009) 926–929, https://doi.org/10.1016/j.jallcom.2008.08.082.

[65] M. Vadivel, R. Ramesh Babu, K. Sethuraman, K. Ramamurthi, M. Arivanandhan, Synthesis, structural, dielectric, magnetic and optical properties of Cr substituted CoFe2O4 nanoparticles by co-precipitation method, J. Magn. Magn. Mater. 362 (2014) 122–129, https://doi.org/10.1016/j.jmmm.2014.03.016.

[66] B.P. Jacob, A. Kumar, R.P. Pant, S. Singh, E.M. Mohammed, Influence of preparation method on structural and magnetic properties of nickel ferrite nanoparticles, Bull. Mater. Sci. 34 (7) (2011) 1345–1350, https://doi.org/10.1007/s12034-011-0326-7.

[67] N.R. Panchal, R.B. Jotania, Cobalt ferrite nano particles by microemulsion route, Nanotechnology. 1 (2010) 17–18.

[68] M. Sakar, S. Balakumar, P. Saravanan, S.N. Jaisankar, Annealing temperature mediated physical properties of bismuth ferrite (BiFeO3) nanostructures synthesized by a novel wet chemical method, Mater. Res. Bull. 48 (8) (2013) 2878–2885, https://doi.org/10.1016/j.materresbull.2013.04.008.

[69] D.C. Bharti, K. Mukherjee, S.B. Majumder, Wet chemical synthesis and gas sensing properties of magnesium zinc ferrite nano-particles, Mater. Chem. Phys. 120 (2-3) (2010) 509–517, https://doi.org/10.1016/j.matchemphys.2009.11.050.

[70] M.A. Ahmed, N. Okasha, S.I. El-Dek, Preparation and characterization of nanometric Mn ferrite via different methods, Nanotechnology. 19 (6) (2008) 065603, https://doi.org/10.1088/0957-4484/19/6/065603.

[71] G.H. An, T.Y. Hwang, J. Kim, J. Kim, N. Kang, S. Kim, Y.M. Choi, Y.H. Choa, Barium hexaferrite nanoparticles with high magnetic properties by salt-assisted ultrasonic spray pyrolysis, J. Alloys Compd. 583 (2014) 145–150, https://doi.org/10.1016/j.jallcom.2013.08.105.

[72] Z. Zhong, Q. Li, Y. Zhang, H. Zhong, M. Cheng, Y. Zhang, Synthesis of nanocrystalline Ni-Zn ferrite powders by refluxing method, Powder Technol. 155 (3) (2005) 193–195, https://doi.org/10.1016/j.powtec.2005.05.060.

[73] L. Zhuang, W. Zhang, Y. Zhao, D. Li, W. Wu, H. Shen, Temperature sensitive ferrofluid composed of Mn 1-xZn xFe 2O 4 nanoparticles prepared by a modified hydrothermal process, Powder Technol. 217 (2012) 46–49, https://doi.org/10.1016/j.powtec.2011.10.007.

[74] G. Fan, Z. Gu, L. Yang, F. Li, Nanocrystalline zinc ferrite photocatalysts formed using the colloid mill and hydrothermal technique, Chem. Eng. J. 155 (1-2) (2009) 534–541, https://doi.org/10.1016/j.cej.2009.08.008.

[75] M. Goodarz Naseri, M.H.M. Ara, E.B. Saion, A.H. Shaari, Superparamagnetic magnesium ferrite nanoparticles fabricated by a simple, thermal-treatment method, J. Magn. Magn. Mater. 350 (2014) 141–147, https://doi.org/10.1016/j.jmmm.2013.08.032.

[76] A. Milutinović, Z. Lazarević, Č. Jovalekić, I. Kuryliszyn-Kudelska, M. Romčević, S. Kostić, N. Romčević, The cation inversion and magnetization in nanopowder zinc ferrite obtained by soft mechanochemical processing, Mater. Res. Bull. 48 (11) (2013) 4759–4768, https://doi.org/10.1016/j.materresbull.2013.08.020.

[77] G. Biasotto, A. Simões, C. Foschini, S. Antônio, M. Zaghete, J. Varela, A novel synthesis of perovskite bismuth ferrite nanoparticles, Process. Appl. Ceram. 5 (3) (2011) 171–179, https://doi.org/10.2298/PAC1103171B.

[78] S. Li, R. Nechache, I.A.V. Davalos, G. Goupil, L. Nikolova, M. Nicklaus, J. Laverdiere, A. Ruediger, F. Rosei, D. Damjanovic, Ultrafast microwave hydrothermal synthesis of BiFeO3 NANOPLATES, J. Am. Ceram. Soc. 96 (10) (2013) 3155–3162, https://doi.org/10.1111/jace:12473.

[79] A.M. Ibrahim, M.M.A. El-Latif, M.M. Mahmoud, Synthesis and characterization of nano-sized cobalt ferrite prepared via polyol method using conventional and microwave heating techniques, J. Alloys Compd. 506 (1) (2010) 201–204, https://doi.org/10.1016/j.jallcom.2010.06.177.

[80] A. Manikandan, L.J. Kennedy, M. Bououdina, J.J. Vijaya, Synthesis, optical and magnetic properties of pure and Co-doped ZnFe 2O4 nanoparticles by microwave combustion method, J. Magn. Magn. Mater. 349 (2014) 249–258, https://doi.org/10.1016/j.jmmm.2013.09.013.

[81] H. Kaur, J. Singh, B.S. Randhawa, Essence of superparamagnetism in cadmium ferrite induced by various organic fuels via novel solution combustion method, Ceram. Int. 40 (8) (2014) 12235–12243, https://doi.org/10.1016/j.ceramint.2014.04.067.

[82] N. Kaur, M. Kaur, Comparative studies on impact of synthesis methods on structural and magnetic properties of magnesium ferrite nanoparticles, Process. Appl. Ceram. 8 (3) (2014) 137–143, https://doi.org/10.2298/PAC1403137K.

[83] R. Sharma, R. Chandra Agarwala, V. Agarwala, A study on the heat-treatments of nanocrystalline nickel substituted BaW hexaferrite produced by low combustion synthesis method, J. Magn. Magn. Mater. 312 (1) (2007) 117–125, https://doi.org/10.1016/j.jmmm.2006.09.021.

[84] A.M. Huízar-Félix, T. Hernández, S. de la Parra, J. Ibarra, B. Kharisov, Sol-gel based Pechini method synthesis and characterization of Sm 1-xCa xFeO 3 perovskite 0.1≤x≤0.5, Powder Technol. 229 (2012) 290–293, https://doi.org/10.1016/j.powtec.2012.06.057.

[85] S.E. Jacobo, C. Herme, P.G. Bercoff, Influence of the iron content on the formation process of substituted Co-Nd strontium hexaferrite prepared by the citrate precursor method, J. Alloys Compd. 495 (2) (2010) 513–515, https://doi.org/10.1016/j.jallcom.2009.10.172.

[86] M.L. Martins, A.O. Florentino, A.A. Cavalheiro, R.I.V. Silva, D.I. Dos Santos, M. J. Saeki, Mechanisms of phase formation along the synthesis of Mn-Zn ferrites by the polymeric precursor method, Ceram. Int. 40 (10) (2014) 16023–16031, https://doi.org/10.1016/j.ceramint.2014.07.137.

[87] A.S. Nikolić, N. Jović, J. Rogan, A. Kremenović, M. Ristić, A. Meden, B. Antić, Carboxylic acids and polyethylene glycol assisted synthesis of nanocrystalline nickel ferrites, Ceram. Int. 39 (6) (2013) 6681–6688, https://doi.org/10.1016/j.ceramint.2013.01.106.

[88] A. Drmota, M. Drofenik, A. Žnidaršič, Synthesis and characterization of nano-crystalline strontium hexaferrite using the co-precipitation and microemulsion methods with nitrate precursors, Ceram. Int. 38 (2) (2012) 973–979, https://doi.org/10.1016/j.ceramint.2011.08.018.

[89] V. Uskoković, M. Drofenik, A mechanism for the formation of nanostructured NiZn ferrites via a microemulsion-assisted precipitation method, Colloids Surfaces A Physicochem. Eng. Asp. 266 (1-3) (2005) 168–174, https://doi.org/10.1016/j.colsurfa.2005.06.022.

[90] S. Tyagi, H.B. Baskey, R.C. Agarwala, V. Agarwala, T.C. Shami, Development of hard/soft ferrite nanocomposite for enhanced microwave absorption, Ceram. Int. 37 (7) (2011) 2631–2641, https://doi.org/10.1016/j.ceramint.2011.04.012.

[91] M.M. Hessien, M.M. Rashad, K. El-Barawy, Controlling the composition and magnetic properties of strontium hexaferrite synthesized by co-precipitation method, J. Magn. Magn. Mater. 320 (3-4) (2008) 336–343, https://doi.org/10.1016/j.jmmm.2007.06.009.

[92] S. Mallesh, M. Vasundhara, V. Srinivas, The Effect of Cationic Disorder on Low Temperature Magnetic Properties of MnZn Ferrite Nanoparticles, IEEE Trans. Magn. 51 (11) (2015) 1–4, https://doi.org/10.1109/TMAG.2015.2440478.

[93] P. Meng, K. Xiong, L. Wang, S. Li, Y. Cheng, G. Xu, Tunable complex permeability and enhanced microwave absorption properties of BaNixCo1-xTiFe10O19, J. Alloys Compd. 628 (2015) 75–80, https://doi.org/10.1016/j.jallcom.2014.10.163.

[94] S. Mallesh, V. Srinivas, A comprehensive study on thermal stability and magnetic properties of MnZn-ferrite nanoparticles, J. Magn. Magn. Mater. 475 (2019) 290–303, https://doi.org/10.1016/j.jmmm.2018.11.052.

[95] S. Mallesh, D. Prabu, V. Srinivas, Thermal stability and magnetic properties of MgFe2O4@ZnO nanoparticles, AIP Adv. 7 (2017) 2–9, https://doi.org/10.1063/1.4975355.

[96] M. Srivastava, A.K. Ojha, S. Chaubey, P.K. Sharma, A.C. Pandey, Influence of pH on structural morphology and magnetic properties of ordered phase cobalt doped lithium ferrites nanoparticles synthesized by sol-gel method, Mater. Sci. Eng. B Solid-State Mater. Adv. Technol. 175 (1) (2010) 14–21, https://doi.org/10.1016/j.mseb.2010.06.005.

[97] X. Huang, J. Zhang, W. Wang, T. Sang, B. Song, H. Zhu, W. Rao, C. Wong, Effect of pH value on electromagnetic loss properties of Co-Zn ferrite prepared via coprecipitation method, J. Magn. Magn. Mater. 405 (2016) 36–41, https://doi.org/10.1016/j.jmmm.2015.12.051.

[98] J. He, L. Deng, H. Luo, L. He, D. Shan, S. Yan, S. Huang, Electromagnetic matching and microwave absorption abilities of Ti3SiC2 encapsulated with Ni0.5Zn0.5Fe2O4 shell, J. Magn. Magn. Mater. 473 (2019) 184–189, https://doi.org/10.1016/j.jmmm.2018.10.061.

[99] N.a. Chen, M. Gu, Microstructure and Microwave Absorption Properties of Y-Substituted Ni-Zn Ferrites, Open J. Met. 02 (02) (2012) 37–41, https://doi.org/10.4236/ojmetal.2012.22006.

[100] F. Tao, M. Green, A.T.V. Tran, Y. Zhang, Y. Yin, X. Chen, Plasmonic Cu9S5 Nanonets for Microwave Absorption, ACS Appl. Nano Mater. 2 (6) (2019) 3836–3847, https://doi.org/10.1021/acsanm.9b0070010.1021/acsanm.9b00700.s001.

[101] Y. Yin, X. Liu, X. Wei, Y.a. Li, X. Nie, R. Yu, J. Shui, Magnetically Aligned Co-C/MWCNTs Composite Derived from MWCNT-Interconnected Zeolitic Imidazolate Frameworks for a Lightweight and Highly Efficient Electromagnetic Wave Absorber, ACS Appl. Mater. Interfaces. 9 (36) (2017) 30850–30861, https://doi.org/10.1021/acsami.7b1006710.1021/acsami.7b10067.s001.

[102] N. Wu, C. Liu, D. Xu, J. Liu, W. Liu, Q. Shao, Z. Guo, Enhanced Electromagnetic Wave Absorption of Three-Dimensional Porous Fe3O4/C Composite Flowers, ACS Sustain. Chem. Eng. 6 (9) (2018) 12471–12480, https://doi.org/10.1021/acssuschemeng.8b03097.

[103] S. Wang, Q. Jiao, Q. Shi, H. Zhu, T. Feng, Q. Lu, C. Feng, H. Li, D. Shi, Y. Zhao, Synthesis of porous nitrogen-doped graphene decorated by γ-Fe2O3 nanorings for enhancing microwave absorbing performance, Ceram. Int. 46 (1) (2020) 1002–1010, https://doi.org/10.1016/j.ceramint.2019.09.064.

[104] R. Shu, J. Zhang, C. Guo, Y. Wu, Z. Wan, J. Shi, Y. Liu, M. Zheng, Facile synthesis of nitrogen-doped reduced graphene oxide/nickel-zinc ferrite composites as high-performance microwave absorbers in the X-band, Chem. Eng. J. 384 (2020) 123266, https://doi.org/10.1016/j.cej.2019.123266.

[105] R. Jaiswal, K. Agarwal, R. Kumar, R. Kumar, K. Mukhopadhyay, N.E. Prasad, EMI and microwave absorbing efficiency of polyaniline-functionalized reduced graphene oxide/γ-Fe2O3/epoxy nanocomposite, Soft Matter. 16 (28) (2020) 6643–6653, https://doi.org/10.1039/D0SM00266F.

[106] A.R. Bueno, M.L. Gregori, M.C.S. Nóbrega, Microwave-absorbing properties of Ni0.50-xZn0.50-x Me2xFe2O4 (Me=Cu, Mn, Mg) ferrite-wax composite in X-band frequencies, J. Magn. Magn. Mater. 320 (6) (2008) 864–870, https://doi.org/10.1016/j.jmmm.2007.09.020.

[107] N. Zinc, F. Pb, Z. Ti, A. Mandal, D. Ghosh, A. Malas, P. Pal, C.K. Das, Synthesis and Microwave Absorbing Properties of Cu-Doped 2013 (2013).

[108] B.Y. Chen, D. Chen, Z.T. Kang, Y.Z. Zhang, Preparation and microwave absorption properties of Ni-Co nanoferrites, J. Alloys Compd. 618 (2015) 222–226, https://doi.org/10.1016/j.jallcom.2014.08.195.

[109] M.A. Almessiere, Y. Slimani, A.V. Trukhanov, A. Demir Korkmaz, S. Guner, S. Akhtar, S.E. Shirsath, A. Baykal, I. Ercan, Effect of Nd-Y co-substitution on structural, magnetic, optical and microwave properties of NiCuZn nanospinel ferrites, J. Mater. Res. Technol. 9 (5) (2020) 11278–11290, https://doi.org/10.1016/j.jmrt.2020.08.027.

[110] M.A. Almessiere, Y. Slimani, B. Unal, T.I. Zubar, A. Sadaqat, A.V. Trukhanov, A. Baykal, Microstructure, dielectric and microwave features of [Ni0.4Cu0.2Zn0.4](Fe2−xTbx)O4 (x ≤ 0.1) nanospinel ferrites, J. Mater. Res. Technol. 9 (2020) 10608–10623, https://doi.org/10.1016/j.jmrt.2020.07.094.

[111] M.A. Almessiere, Y. Slimani, H. Güngüneş, V.G. Kostishyn, S.V. Trukhanov, A. V. Trukhanov, A. Baykal, Impact of Eu3+ ion substitution on structural, magnetic and microwave traits of Ni–Cu–Zn spinel ferrites, Ceram. Int. 46 (8) (2020) 11124–11131, https://doi.org/10.1016/j.ceramint.2020.01.132.

[112] M.A. Almessiere, Y. Slimani, A.V. Trukhanov, A. Baykal, H. Gungunes, E. L. Trukhanova, S.V. Trukhanov c, V.G. Kostishin, Strong correlation between Dy3 + concentration, structure, magnetic and microwave properties of the [Ni0.5Co0.5](DyxFe2-x)O4 nanosized ferrites, J. Ind. Eng. Chem. 90 (2020) 251–259, https://doi.org/10.1016/j.jiec.2020.07.020.

[113] K. Shi, J. Li, S. He, H. Bai, Y. Hong, Y. Wu, D. Jia, Z. Zhou, A superior microwave absorption material: Ni2+-Zr4+ Co-Doped barium ferrite ceramics with large reflection loss and broad bandwidth, Curr. Appl. Phys. 19 (7) (2019) 842–848, https://doi.org/10.1016/j.cap.2019.03.018.

[114] Y. Feng, X. Guo, H. Gong, Y. Zhang, Y.u. Liu, X. Lin, J. Mao, Microwave absorption performance of PDCs-SiCN(Fe) ceramics with negative imaginary permeability, Ceram. Int. 44 (9) (2018) 10420–10425, https://doi.org/10.1016/j.ceramint.2018.03.058.

[115] Y. Wang, X. Guo, Y. Feng, X. Lin, H. Gong, Wave absorbing performance of polymer-derived SiCN(Fe) ceramics, Ceram. Int. 43 (17) (2017) 15551–15555, https://doi.org/10.1016/j.ceramint.2017.08.106.

[116] Y. Wang, Y. Feng, X. Guo, Y.u. Liu, H. Gong, Electromagnetic and wave absorbing properties of Fe-doped polymer-derived SiCN ceramics, RSC Adv. 7 (73) (2017) 46215–46220, https://doi.org/10.1039/C7RA09399C.

[117] Y.u. Liu, Y. Feng, H. Gong, X. Guo, X. Lin, B. Xie, Y. Zhang, Electromagnetic wave absorption properties of europium-doped SiCN (Fe) polymer-derived ceramics, J. Mater. Sci. Mater. Electron. 29 (14) (2018) 12496–12502, https://doi.org/10.1007/s10854-018-9368-6.

[118] Y. Liu, Y. Feng, H. Gong, Y. Zhang, X. Lin, B. Xie, J. Mao, Microwave absorbing performance of polymer-derived SiCN (Ni) ceramics prepared from different nickel sources, J. Alloys Compd. 749 (2018) 620–627, https://doi.org/10.1016/j.jallcom.2018.03.346.

[119] S. Singh, S. Shukla, A. Kumar, D. Singh, Influence of Zn dispersion in SiC on electromagnetic wave absorption characteristics, J. Alloys Compd. 738 (2018) 448–460, https://doi.org/10.1016/j.jallcom.2017.12.190.

[120] S. Singh, A. Sinha, R.H. Zunke, A. Kumar, D. Singh, Double layer microwave absorber based on Cu dispersed SiC composites, Adv. Powder Technol. 29 (9) (2018) 2019–2026, https://doi.org/10.1016/j.apt.2018.05.008.

[121] O.A. Elkady, S.A. Abolkassem, A.H. Elsayed, W.A. Hussein, K.F.A. Hussein, Microwave absorbing efficiency of Al matrix composite reinforced with nano-Ni/SiC particles, Results Phys. 12 (2019) 687–700, https://doi.org/10.1016/j.rinp.2018.11.095.
[122] S.H. Hosseini, A. Asadnia, Synthesis, characterization, and microwave-absorbing properties of polypyrrole/MnFe 2O 4 nanocomposite, J. Nanomater. 2012 (2012), https://doi.org/10.1155/2012/198973.
[123] N.Y. Mostafa, M.M. Hessien, A.A. Shaltout, Hydrothermal synthesis and characterizations of Ti substituted Mn-ferrites, J. Alloys Compd. 529 (2012) 29–33, https://doi.org/10.1016/j.jallcom.2012.03.060.
[124] C.-H. Peng, C.-C. Hwang, J. Wan, J.-S. Tsai, S.-Y. Chen, Microwave-absorbing characteristics for the composites of thermal-plastic polyurethane (TPU)-bonded NiZn-ferrites prepared by combustion synthesis method, Mater. Sci. Eng. B Solid-State Mater. Adv. Technol. 117 (1) (2005) 27–36, https://doi.org/10.1016/j.mseb.2004.10.022.
[125] Z.-H. Liu, R. Tao, P. Luo, X. Shu, G.-D. Ban, Preparation and microwave absorbing property of carbon fiber/polyurethane radar absorbing coating, RSC Adv. 7 (73) (2017) 46060–46068, https://doi.org/10.1039/C7RA07666E.
[126] M. Saini, S.K. Singh, R. Shukla, A. Kumar, Mg Doped Copper Ferrite with Polyaniline Matrix Core-Shell Ternary Nanocomposite for Electromagnetic Interference Shielding, J. Inorg. Organomet. Polym. Mater. 28 (6) (2018) 2306–2315, https://doi.org/10.1007/s10904-018-0907-7.
[127] R.T. Ma, H.T. Zhao, G. Zhang, Preparation, characterization and microwave absorption properties of polyaniline/Co0.5Zn0.5Fe2O4 nanocomposite, Mater. Res. Bull. 45 (9) (2010) 1064–1068, https://doi.org/10.1016/j.materresbull.2010.06.021.
[128] S.M. Abbas, A.K. Dixit, R. Chatterjee, T.C. Goel, Complex permittivity, complex permeability and microwave absorption properties of ferrite-polymer composites, J. Magn. Magn. Mater. 309 (1) (2007) 20–24, https://doi.org/10.1016/j.jmmm.2006.06.006.
[129] T. Liu, N. Liu, S. Zhai, S. Gao, Z. Xiao, Q. An, D. Yang, Tailor-made core/shell/shell-like Fe3O4@SiO2@PPy composites with prominent microwave absorption performance, J. Alloys Compd. 779 (2019) 831–843, https://doi.org/10.1016/j.jallcom.2018.11.167.
[130] B. Li, X. Weng, G. Wu, Y. Zhang, X. Lv, G. Gu, Synthesis of Fe3O4/polypyrrole/polyaniline nanocomposites by in-situ method and their electromagnetic absorbing properties, J. Saudi Chem. Soc. 21 (4) (2017) 466–472, https://doi.org/10.1016/j.jscs.2016.11.005.
[131] Y. lei, Z. Yao, H. Lin, J. Zhou, A.A. Haidry, P. liu, The effect of polymerization temperature and reaction time on microwave absorption properties of Co-doped ZnNi ferrite/polyaniline composites, RSC Adv. 8 (51) (2018) 29344–29355, https://doi.org/10.1039/C8RA05500A.
[132] K. Manna, S.K. Srivastava, Fe3O4@Carbon@Polyaniline Trilaminar Core-Shell Composites as Superior Microwave Absorber in Shielding of Electromagnetic Pollution, ACS Sustain. Chem. Eng. 5 (11) (2017) 10710–10721, https://doi.org/10.1021/acssuschemeng.7b0268210.1021/acssuschemeng.7b02682.s001.
[133] P. Xiong, H. Huang, X. Wang, Design and synthesis of ternary cobalt ferrite/graphene/polyaniline hierarchical nanocomposites for high-performance supercapacitors This work is dedicated to Professor MIN Enze on the occasion of his 90th birthday, J. Power Sources. 245 (2014) 937–946, https://doi.org/10.1016/j.jpowsour.2013.07.064.
[134] M. Kwiatkowski, A. Policicchio, M. Seredych, T.J. Bandosz, Evaluation of CO2 interactions with S-doped nanoporous carbon and its composites with a reduced GO: Effect of surface features on an apparent physical adsorption mechanism, Carbon N. Y. 98 (2016) 250–258, https://doi.org/10.1016/j.carbon.2015.11.019.
[135] K. Mondal, B. Balasubramaniam, A. Gupta, A.A. Lahcen, M. Kwiatkowski, Carbon Nanostructures for Energy and Sensing Applications, J. Nanotechnol. 2019 (2019) 10–13, https://doi.org/10.1155/2019/1454327.
[136] L.J. Yu, S.H. Ahmad, I. Kong, M.A. Tarawneh, Microwave absorbing properties of nickel-zinc ferrite/multiwalled nanotube thermoplastic natural rubber composites, Adv. Mater. Res. 501 (2012) 24–28, https://doi.org/10.4028/www.scientific.net/AMR.501.24.
[137] X. Liu, H. Guo, Q. Xie, Q. Luo, L. Sen Wang, D.L. Peng, Enhanced microwave absorption properties in GHz range of Fe3O4/C composite materials, J. Alloys Compd. 649 (2015) 537–543, https://doi.org/10.1016/j.jallcom.2015.07.084.
[138] X. Liu, Y. Ma, Q. Zhang, Z. Zheng, L. Sen Wang, D.L. Peng, Facile synthesis of Fe 3 O 4 /C composites for broadband microwave absorption properties, Appl. Surf. Sci. 445 (2018) 82–88, https://doi.org/10.1016/j.apsusc.2018.03.127.
[139] A. Feng, T. Hou, Z. Jia, G. Wu, Synthesis of a hierarchical carbon fiber@cobalt ferrite@manganese dioxide composite and its application as a microwave absorber, RSC Adv. 10 (18) (2020) 10510–10518, https://doi.org/10.1039/C9RA10327A.
[140] P. Liu, Y. Huang, J. Yan, Y. Yang, Y. Zhao, Construction of CuS Nanoflakes Vertically Aligned on Magnetically Decorated Graphene and Their Enhanced Microwave Absorption Properties, ACS Appl. Mater. Interfaces. 8 (8) (2016) 5536–5546, https://doi.org/10.1021/acsami.5b10511.
[141] N.a. Zhang, Y. Huang, M. Zong, X. Ding, S. Li, M. Wang, Coupling CoFe2O4 and SnS2 nanoparticles with reduced graphene oxide as a high-performance electromagnetic wave absorber, Ceram. Int. 42 (14) (2016) 15701–15708, https://doi.org/10.1016/j.ceramint.2016.07.028.
[142] M. Zong, Y. Huang, H. Wu, Y. Zhao, Q. Wang, X. Sun, One-pot hydrothermal synthesis of RGO/CoFe2O4 composite and its excellent microwave absorption properties, Mater. Lett. 114 (2014) 52–55, https://doi.org/10.1016/j.matlet.2013.09.113.
[143] J. Li, Y. Xie, W. Lu, T.W. Chou, Flexible electromagnetic wave absorbing composite based on 3D rGO-CNT-Fe3O4 ternary films, Carbon N. Y. 129 (2018) 76–84, https://doi.org/10.1016/j.carbon.2017.11.094.
[144] R. Bhattacharyya, O.m. Prakash, S. Roy, A.P. Singh, T.K. Bhattacharya, P. Maiti, S. Bhattacharyya, S. Das, Graphene oxide-ferrite hybrid framework as enhanced broadband absorption in gigahertz frequencies 9 (1) (2019), https://doi.org/10.1038/s41598-019-48487-5.
[145] J. Li, D. Zhou, W. Liu, J. Su, M. Fu, Scripta Materialia Novel and facile reduced graphene oxide anchored Ni-Co-Zn-Nd-ferrites composites for microwave absorption, Scr. Mater. 171 (2019) 42–46, https://doi.org/10.1016/j.scriptamat.2019.06.018.
[146] S. Acharya, P. Alegaonkar, S. Datar, microwave absorption properties of the composite, Chem. Eng. J. 374 (2019) 144–154, https://doi.org/10.1016/j.cej.2019.05.078.
[147] S. Ni, S. Lin, Q. Pan, F. Yang, K. Huang, D. He, Hydrothermal synthesis and microwave absorption properties of Fe 3O4 nanocrystals, J. Phys. D. Appl. Phys. 42 (5) (2009) 055004, https://doi.org/10.1088/0022-3727/42/5/055004.
[148] S. Ni, X. Sun, X. Wang, G. Zhou, F. Yang, J. Wang, D. He, Low temperature synthesis of Fe3O4 micro-spheres and its microwave absorption properties, Mater. Chem. Phys. 124 (1) (2010) 353–358, https://doi.org/10.1016/j.matchemphys.2010.06.046.
[149] A. Yan, Y. Liu, Y. Liu, X. Li, Z. Lei, P. Liu, A NaAc-assisted large-scale coprecipitation synthesis and microwave absorption efficiency of Fe 3O 4 nanowires, Mater. Lett. 68 (2012) 402–405, https://doi.org/10.1016/j.matlet.2011.10.093.
[150] Z. Zou, A.G. Xuan, Z.G. Yan, Y.X. Wu, N. Li, Preparation of Fe3O4 particles from copper/iron ore cinder and their microwave absorption properties, Chem. Eng. Sci. 65 (1) (2010) 160–164, https://doi.org/10.1016/j.ces.2009.06.003.
[151] X. Li, X. Han, Y. Tan, P. Xu, Preparation and microwave absorption properties of Ni-B alloy-coated Fe3O4 particles, J. Alloys Compd. 464 (1-2) (2008) 352–356, https://doi.org/10.1016/j.jallcom.2007.09.123.
[152] D.-L. Zhao, Q. Lv, Z.-M. Shen, Fabrication and microwave absorbing properties of Ni-Zn spinel ferrites, J. Alloys Compd. 480 (2) (2009) 634–638, https://doi.org/10.1016/j.jallcom.2009.01.130.
[153] H. Bayrakdar, Complex permittivity, complex permeability and microwave absorption properties of ferrite-paraffin polymer composites, J. Magn. Magn. Mater. 323 (14) (2011) 1882–1885, https://doi.org/10.1016/j.jmmm.2011.02.030.
[154] Y. Li, H.J. Yang, W.G. Yang, Z.L. Hou, J.B. Li, H.B. Jin, J. Yuan, M.S. Cao, Structure, ferromagnetism and microwave absorption properties of la substituted BiFeO3 nanoparticles, Mater. Lett. 111 (2013) 130–133, https://doi.org/10.1016/j.matlet.2013.08.061.
[155] M. Du, Z. Yao, J. Zhou, P. Liu, T. Yao, R. Yao, Design of efficient microwave absorbers based on multi-layered polyaniline nanofibers and polyaniline nanofibers/Li0.35Zn0.3Fe2.35O4 nanocomposite, Synth. Met. 223 (2017) 49–57, https://doi.org/10.1016/j.synthmet.2016.11.039.
[156] M. Wang, G. Ji, B. Zhang, D. Tang, Y. Yang, Y. Du, Controlled synthesis and microwave absorption properties of Ni0.6Zn0.4Fe2O4/PANI composite via an in-situ polymerization process, J. Magn. Magn. Mater. 377 (2015) 52–58, https://doi.org/10.1016/j.jmmm.2014.10.066.
[157] Y. Cheng, H. Zhao, Z. Yang, J. Lv, J. Cao, X. Qi, G. Ji, Y. Du, An unusual route to grow carbon shell on Fe3O4 microspheres with enhanced microwave absorption, J. Alloys Compd. 762 (2018) 463–472, https://doi.org/10.1016/j.jallcom.2018.05.261.
[158] T. Wu, Y. Liu, X. Zeng, T. Cui, Y. Zhao, Y. Li, G. Tong, Facile Hydrothermal Synthesis of Fe3O4/C Core-Shell Nanorings for Efficient Low-Frequency Microwave Absorption, ACS Appl. Mater. Interfaces. 8 (11) (2016) 7370–7380, https://doi.org/10.1021/acsami.6b0026410.1021/acsami.6b00264.s001.
[159] P. Yin, Y.u. Deng, L. Zhang, J. Huang, H. Li, Y. Li, Y. Qi, Y.u. Tao, The microwave absorbing properties of ZnO/Fe3O4/paraffin composites in low frequency band, Mater. Res. Express. 5 (2) (2018) 026109, https://doi.org/10.1088/2053-1591/aaae58.
[160] Z. Han, D.a. Li, X. Liu, D. Geng, J.i. Li, Z. Zhang, Microwave-absorption properties of Fe(Mn)/ferrite nanocapsules, J. Phys. D. Appl. Phys. 42 (5) (2009) 055008, https://doi.org/10.1088/0022-3727/42/5/055008.
[161] P. Meng, K. Xiong, K. Ju, S. Li, G. Xu, Wideband and enhanced microwave absorption performance of doped barium ferrite, J. Magn. Magn. Mater. 385 (2015) 407–411, https://doi.org/10.1016/j.jmmm.2015.02.059.
[162] W. Chen, J. Zheng, Y. Li, Synthesis and electromagnetic characteristics of BaFe 12O 19/ZnO composite material, J. Alloys Compd. 513 (2012) 420–424, https://doi.org/10.1016/j.jallcom.2011.10.060.
[163] S. Chang, S. Kangning, C. Pengfei, Microwave absorption properties of Ce-substituted M-type barium ferrite, J. Magn. Magn. Mater. 324 (5) (2012) 802–805, https://doi.org/10.1016/j.jmmm.2011.09.023.
[164] R. Shu, G. Zhang, J. Zhang, X. Wang, M. Wang, Y. Gan, J. Shi, J. He, Synthesis and high-performance microwave absorption of reduced graphene oxide/zinc ferrite hybrid nanocomposite, Mater. Lett. 215 (2018) 229–232, https://doi.org/10.1016/j.matlet.2017.12.108.
[165] M. Zong, Y. Huang, X. Ding, N.a. Zhang, C. Qu, Y. Wang, One-step hydrothermal synthesis and microwave electromagnetic properties of RGO/NiFe2O4 composite, Ceram. Int. 40 (5) (2014) 6821–6828, https://doi.org/10.1016/j.ceramint.2013.11.145.
[166] M. Zong, Y. Huang, N. Zhang, Reduced graphene oxide-CoFe 2 O 4 composite: Synthesis and electromagnetic absorption properties, Appl. Surf. Sci. 345 (2015) 272–278, https://doi.org/10.1016/j.apsusc.2015.03.203.

[167] P. Liu, Y. Huang, X. Zhang, Cubic NiFe2O4 particles on graphene-polyaniline and their enhanced microwave absorption properties, Compos. Sci. Technol. 107 (2015) 54–60, https://doi.org/10.1016/j.compscitech.2014.11.021.
[168] M.S. Mustaffa, R.S. Azis, N.H. Abdullah, I. Ismail, I.R. Ibrahim, An investigation of microstructural, magnetic and microwave absorption properties of multi-walled carbon nanotubes/Ni0.5Zn0.5Fe2O4, Sci. Rep. 9 (2019) 3–9, https://doi.org/10.1038/s41598-019-52233-2.
[169] W. Ye, Q. Sun, X. Long, Y. Cai, Preparation and properties of CF-Fe3O4-BN composite electromagnetic wave-absorbing materials, RSC Adv. 10 (19) (2020) 11121–11131, https://doi.org/10.1039/D0RA00785D.